JCI The Journal of Clinical Investigation

Fbxw7 increases CCL2/7 in CX3CR1^{hi} macrophages to promote intestinal inflammation

Jia He, … , Lihua Lai, Qingqing Wang

J Clin Invest. 2019. https://doi.org/10.1172/JCI123374.

Research In-Press Preview **Immunology** **Inflammation**

Resident and inflammatory mononuclear phagocytes (MPh) with functional plasticity in the intestine are critically involved in the pathology of Inflammatory Bowel Diseases (IBD), in which the mechanism remains incompletely understood. In the present study, we found that increased expression of E3 ligase FBXW7 in the inflamed intestine was significantly correlated to IBD severity in both human diseases and mice model. Myeloid-*Fbxw7* deficiency protected mice from dextran sodium sulfate (DSS) and 2,6,4-trinitrobenzene sulfonic acid (TNBS) induced colitis. *Fbxw7* deficiency resulted in decreased production of chemokines CCL2 and CCL7 by colonic CX3CR1^{hi} resident macrophages and reduced accumulation of CX3CR1^{int} pro-inflammatory MPh in colitis colon tissue. Mice received AAV-shFbxw7 administration showed significantly improved survival rate and alleviated colitis. Mechanisms screening demonstrated that FBXW7 suppresses H3K27me3 modification and promotes *Ccl2* and *Ccl7* expression via degradation of histone-lysine N-methyltransferase EZH2 in macrophages. Taken together, our results indicate that FBXW7 degrades EZH2 and increases *Ccl2/Ccl7* in CX3CR1^{hi} macrophages, which promotes the recruiting CX3CR1^{int} pro-inflammatory MPh into local colon tissues with colitis. Targeting FBXW7 might represent a potential therapeutic approach for intestine inflammation intervention.

Fbxw7 increases CCL2/7 in CX3CR1^{hi} macrophages to promote intestinal inflammation

Jia He[1,#], Yinjing Song[1,#], Gaopeng Li[1,#], Peng Xiao[2], Yang Liu[1], Yue Xue[1], Qian Cao[2], Xintao Tu[1], Ting Pan[1], Zhinong Jiang[3], Xuetao Cao[1,4], Lihua Lai[1,*], and Qingqing Wang[1,*]

Authors Affiliations

[1]Institute of Immunology, Zhejiang University School of Medicine, Hangzhou 310058, Zhejiang, P. R. China. [2]Department of Gastroenterology, Sir Run Run Shaw Hospital, Zhejiang University School of Medicine, Hangzhou 310020, Zhejiang, P. R. China. [3]Department of Pathology, Sir Run Run Shaw Hospital, Zhejiang University School of Medicine, Hangzhou 310020, Zhejiang, P. R. China. [4]National Key Laboratory of Medical Molecular Biology, Institute of Basic Medical Sciences, Peking Union Medical College, Chinese Academy of Medical Sciences, Beijing 100730, P. R. China.

[#] These authors contributed equally

***Corresponding Author:** Qingqing Wang or Lihua Lai, Institute of Immunology, Zhejiang University School of Medicine, 866 Yu Hang Tang Road, Hangzhou 310058, Zhejiang, P. R. China, Phone: +86-571-88208284, Fax: +86-571-88208285, E-mail: wqq@zju.edu.cn, lailihua@zju.edu.cn

Conflicts of Interest

The authors have declared that no conflict of interest exists.

Abstract

Resident and inflammatory mononuclear phagocytes (MPh) with functional plasticity in the intestine are critically involved in the pathology of Inflammatory Bowel Diseases (IBD), in which the mechanism remains incompletely understood. In the present study, we found that increased expression of E3 ligase FBXW7 in the inflamed intestine was significantly correlated to IBD severity in both human diseases and mice model. Myeloid-*Fbxw7* deficiency protected mice from dextran sodium sulfate (DSS) and 2,6,4-trinitrobenzene sulfonic acid (TNBS) induced colitis. *Fbxw7* deficiency resulted in decreased production of chemokines CCL2 and CCL7 by colonic CX3CR1^{hi} resident macrophages and reduced accumulation of CX3CR1^{int} pro-inflammatory MPh in colitis colon tissue. Mice received AAV-shFbxw7 administration showed significantly improved survival rate and alleviated colitis. Mechanisms screening demonstrated that FBXW7 suppresses H3K27me3 modification and promotes *Ccl2* and *Ccl7* expression via degradation of histone-lysine N-methyltransferase EZH2 in macrophages. Taken together, our results indicate that FBXW7 degrades EZH2 and increases *Ccl2/Ccl7* in CX3CR1^{hi} macrophages, which promotes the recruiting CX3CR1^{int} pro-inflammatory MPh into local colon tissues with colitis. Targeting FBXW7 might represent a potential therapeutic approach for intestine inflammation intervention.

Introduction

Chronic and progressive inflammation is the key pathogenesis of inflammatory bowel disease (IBD) including Crohn's disease (CD) and ulcerative colitis (UC), in which dysregulation of the genetic, environmental or microbial factors and immune responses is involved. Macrophages induced innate immune response within the intestinal mucosa was the first line against the invading pathogens (1-3). Inefficient or over activation of gastrointestinal macrophage subsets participate in IBD development by regulating the initiation, amplification and resolution of local inflammation (4-6).

Monocyte-derived mononuclear phagocytes (MPh) in colonic lamina propria (CLP) express certain levels of the chemokine CX3C receptor (CX3CR)1, and CD11b (7,8). In a healthy colon, Ly6C^{hi} (Ly6C high-positive) monocytes mainly give rise to CX3CR1^{hi} (CX3CR1 high-positive) resident macrophages that contribute to the maintenance of gut homeostasis and protect the host from certain pathogens (9,10). However, the phenotype and fate of mucosal monocyte-derived MPh change dramatically in inflammation environments. Under these circumstances, CX3CR1^{hi} resident macrophages that dominate in the healthy colon are replaced by inflammation elicited plastic CX3CR1^{int} (CX3CR1 intermediate-positive) mononuclear phagocytes (MPh) that are the progeny of rapidly infiltrating Ly6C^{hi} circulating peripheral blood monocytes (11), which express higher levels of pro-inflammatory mediators and toll-like receptors, nitric oxide, reactive oxygen intermediates, cathepsins and metalloproteases than their resident counterparts, forming an intense infiltration in CLP. As a result, CX3CR1^{int} pro-inflammatory MPh aggravate intestinal inflammatory response and play crucial roles in the pathogenesis of CD and UC (7). Although the cells in this MPh pool are on a differentiation waterfall that may include populations that have predominantly more macrophage-like functions, there are also a small number of cells with DC-like functions (10). So, we call CLP CX3CR1^{int} MPh instead of CX3CR1^{int} macrophages in the article.

The infiltrations of CX3CR1^{int} pro-inflammatory MPh can be triggered by dysregulated expression of chemokines in inflamed colon tissues through recruitment of Ly6C^{hi} monocytes which differentiate into CX3CR1^{int} pro-inflammatory MPh and produce

pro-inflammatory cytokines including IL-6 and TNF-α (12,13). Chemokines are produced by a wide variety of cells, including the inflammatory cells present in IBD lesions, fibroblasts, endothelial and epithelial cells in the gastrointestinal system. The potent capacity to secret chemokines by macrophages to mediate immune cell recruitment has been demonstrated in previous studies, which is critical for inflammation cascade (14-16). It has been reported that the increase of inflammatory macrophages in anti-TNF-α non-responding IBD patients is associated with the upregulation of TREM-1/CCL7/CCR2 axis (17). The induction of chemokines has been reported via activation of the NF-κB signaling cascade (18-20), however mechanisms by which the complex cytokine and chemokine network in colonic microenvironment influences the inflammatory MPh infiltration are not well defined and represent a fundamental gap in the understanding of homeostatic immune function and IBD development.

FBXW7 (F-box and WD repeat domain-containing 7) is a component of SCF (complex of SKP1, CUL1 and F-box protein) type ubiquitin ligase. *Fbxw7* mutations have been identified in various types of cancers (21). FBXW*7* is also reported to regulate lipid metabolism (22), target osteogenic and chondrogenic transcriptional factors (23), interact with parkin and play important roles in Parkinson's disease (24). Our previous study has identified that FBXW7 is critical in promoting innate antiviral immunity by mediating the ubiquitination of SHP2 (25). However, the function and mechanisms of FBXW7 in inflammation responses has not been clarified. In this study, we found that FBXW7 expression was significantly increased in inflamed intestine tissues from patients with UC and CD. *Fbxw7* deficiency in myeloid cells reduced inflammation and disease severity in colitis mouse model. FBXW7 promoted enhancer of zeste homolog 2 (EZH2) ubiquitination and decreased the H3K27me3 modification on the promoters of chemokines *Ccl2/Ccl7*. Increased *Fbxw7* expression exacerbates colitis by promoting degradation of EZH2 and increasing CCL2/7 in $CX3CR1^{hi}$ macrophages. FBXW7/EZH2/CCL2/7 pathway induces the severity of colitis through recruiting $CX3CR1^{int}$ pro-inflammatory MPh and FBXW7 may serve as a new diagnostic marker and potential therapeutic target for IBD.

Results

Increased FBXW7 expression in IBD

We first analyzed the expression level of *FBXW7* in colonic mucosa samples with or without signs of inflammation from patients with ulcerative colitis (UC) in the GEO database. Compared with healthy mucosa, the expression of *FBXW7* was significantly increased in the active UC mucosa, while to a lesser extent in the inactive UC mucosa (supplementary figure S1A). Moreover, the expression of FBXW7 in colon tissue macrophages observed by immunohistochemical and immunofluorescence staining (figure 1A-B) and mRNA expression of *FBXW7* in peripheral blood monocytes (figure 1C) were markedly increased in IBD patients compared with healthy control subjects or non-IBD inflammatory controls (acute diarrheas). *FBXW7* mRNA level in peripheral blood monocytes was significantly higher in UC patients (supplementary figure S1B) and CD patients (supplementary figure S1C) with severe colitis than in those with mild colitis or in healthy controls. However, the expression of *FBXW7* has no difference in peripheral blood lymphocytes between IBD cases and controls (figure 1D).

The expression of FBXW7 in $CD11b^{+}CX3CR1^{+}$ CLP macrophages (figure 2A-B) was significantly increased in DSS-induced colitis mouse model or in interleukin 10 gene knockout (*Il-10*$^{-/-}$) mice, and *Fbxw7* mRNA expression in peripheral blood monocytes of mice (figure 2C) showed a progressive increase upon DSS challenge. FBXW7 expression in $Ly6C^{hi}$ colonic monocytes was also dramatically increased (figure 2D). Moreover, immunofluorescence staining confirmed an upregulation of FBXW7 expression in colonic $CD68^{+}$ macrophages (figure 2E) and $F4/80^{+}$ macrophages (figure 2F) after DSS treatment for 5 days compared with those in the healthy colon of mice. These results suggest that increased FBXW7 expression in monocytes/macrophages was correlated with local colonic inflammation in both human and mice.

Fbxw7 deficiency attenuated experimental colitis

To investigate the role of *Fbxw7* in macrophages in colitis, LysM-cre^{+} *Fbxw7*$^{f/f}$ (*LysM*$^{+}$*Fbxw7*$^{f/f}$) mice and their control littermates (*Fbxw7*$^{f/f}$) were subjected to acute colitis

model by using 3% DSS. Colitis-induced macroscopic changes (body weight loss, diarrhea and rectal bleeding) were significantly alleviated in *LysM*$^{+}$*Fbxw7*$^{f/f}$ mice compared with those in *Fbxw7*$^{f/f}$ littermates (figure 3A). *LysM*$^{+}$*Fbxw7*$^{f/f}$ mice sacrificed on day 9 displayed significantly longer colons (figure 3B), milder epithelial damage and deceased area of mucosal ulceration (figure 3C and supplementary figure S2A) compared with *Fbxw7*$^{f/f}$ littermates. Moreover, the expression levels of tight junction genes, the mRNA of *Cldn1/2, Ocln* and *Tjp1* (supplementary figure S2B) and the protein of TJP1 (supplementary figure S2C) were significantly higher in the epithelium of *LysM*$^{+}$*Fbxw7*$^{f/f}$ mice compared with that in *Fbxw7*$^{f/f}$ littermates after DSS treatment, which indicated that the epithelial barrier integrity was less disrupted in myeloid *Fbxw7* deficient mice during colonic inflammation. Simultaneously, *LysM*$^{+}$*Fbxw7*$^{f/f}$ mice showed significantly improved survival rate compared with *Fbxw7*$^{f/f}$ littermates after 4% DSS treatment (figure 3D), indicating that *Fbxw7* deficiency protects mice from DSS-induced colitis.

During the recovery period of intestinal inflammation, the rate of body weight gain was more rapid in *LysM*$^{+}$*Fbxw7*$^{f/f}$ mice than that in *Fbxw7*$^{f/f}$ littermates (figure 3E). Moreover, *LysM*$^{+}$*Fbxw7*$^{f/f}$ mice showed longer colon length than *Fbxw7*$^{f/f}$ littermates (figure 3F) on day 15. Similarly, TNBS induced colon shortening, disease activity index, body weight loss and epithelial damage were also alleviated in *LysM*$^{+}$*Fbxw7*$^{f/f}$ mice compared with *Fbxw7*$^{f/f}$ littermates (supplementary figure S3A-D). Above data indicate that myeloid *Fbxw7* deficiency attenuated experimental colitis.

Fbxw7 deficiency decreases the accumulation of pro-inflammatory MPh

Microbiota-induced inflammation is critical for the regulation of intestinal homeostasis. To determine whether decreased DSS colitis susceptibility in *LysM*$^{+}$*Fbxw7*$^{f/f}$ mice was mediated by the shifts of gut microbiota, we analyzed the fecal microbiota composition in *LysM*$^{+}$*Fbxw7*$^{f/f}$ mice and *Fbxw7*$^{f/f}$ littermates. The relative abundance of bacteria at the phylum level and species composition according to OTUs (Operational Taxonomic Units) cluster between *LysM*$^{+}$*Fbxw7*$^{f/f}$ mice and *Fbxw7*$^{f/f}$ littermates was shown in supplementary figure S4A and figure 4A. Moreover, microbial community diversity (figure 4B) and

microbial community composition (supplementary figure S4B) have no significant difference between *LysM*$^{+}$*Fbxw7*$^{f/f}$ mice and *Fbxw7*$^{f/f}$ littermates. Furthermore, we transferred fecal microbiota from *LysM*$^{+}$*Fbxw7*$^{f/f}$ mice to *Fbxw7*$^{f/f}$ mice by cohousing, at the end of colitis period, cohoused-*LysM*$^{+}$*Fbxw7*$^{f/f}$ mice still showed clear alleviation of DSS-induced colitis (supplementary figure S4C-G) compared with cohoused *Fbxw7*$^{f/f}$ or single housed *Fbxw7*$^{f/f}$ mice. These results demonstrated that decreased DSS colitis susceptibility in *LysM*$^{+}$*Fbxw7*$^{f/f}$ mice was not due to the change of microbiome.

We next investigated the changes of myeloid cell subpopulations in CLP during colitis development by analyzing CD11b^{+}CX3CR1^{hi} resident macrophages and CD11b^{+}CX3CR1^{int} pro-inflammatory MPh in a colon. We found that the accumulation of CX3CR1^{int} pro-inflammatory MPh (red) increased with the severity of intestinal inflammation and finally reached its highest proportion at day 9 after DSS treatment in WT mice (*Fbxw7*$^{f/f}$) (figure 4C-D). Importantly, KO mice (*LysM*$^{+}$*Fbxw7*$^{f/f}$) showed obviously reduced accumulation of this CX3CR1^{int} population compared with *Fbxw7*$^{f/f}$ littermates starting from the third day after DSS treatment, but the frequency of CX3CR1^{hi} resident macrophages (blue) in *LysM*$^{+}$*Fbxw7*$^{f/f}$ and *Fbxw7*$^{f/f}$ littermates showed no significant difference during the colitis (figure 4C-D). In addition, the percentage and number of Ly6C^{hi}CX3CR1^{int} monocytes (figure 4E), and percentage of CD11b^{+}Ly6G^{+} neutrophils in CLP (supplementary figure S5A) were lower in *LysM*$^{+}$*Fbxw7*$^{f/f}$ mice than those in *Fbxw7*$^{f/f}$ mice at the later, but not early stage of colitis, while the accumulation of CD103^{+} or CD103^{-} DCs was similar in CLP of *LysM*$^{+}$*Fbxw7*$^{f/f}$ mice and *Fbxw7*$^{f/f}$ littermates (supplementary figure S5B).

Neutrophils also express a high level of *Lyz2* and can be recruited to inflamed tissue to exert antimicrobial activities, the expression of FBXW7 was also increased in peripheral blood and CLP neutrophils from colitis mice compared with healthy mice (supplementary figure S6A-B). We then investigated whether the attenuated colitis in *LysM*$^{+}$*Fbxw7*$^{f/f}$ mice was related to the neutrophils. Depletion of neutrophils by anti-Ly6G antibody could not abrogate the reduced inflammation phenotype of *LysM*$^{+}$*Fbxw7*$^{f/f}$ mice (supplementary

figure S6C-G). These findings indicated that the function of *Fbxw7* in colitis was not dependent on neutrophils.

To further confirm that the function of *Fbxw7* in colitis was dependent on macrophages, we depleted macrophages using clodronate-containing liposomes (CLs) (26,27). Flow cytometry analysis confirmed a marked reduction in the percentages of local macrophages in mice treated with CLs (supplementary figure S7A-B). The protective effect of myeloid deficiency of *Fbxw7* in colitis disappeared in the absence of macrophages compared to the control cohort (figure 4F-I), which was further confirmed by tight junction protein expression (supplementary figure S7C) as well as the production of inflammatory cytokines during colonic inflammation (supplementary figure S7D). We also confirmed the increased *Fbxw7* expression in sorted CX3CR1^{hi} resident macrophages and CX3CR1^{int} MPh from DSS-induced colitis C57BL/6 mice compared with that in healthy control mice (supplementary figure S7E).

Taken together, these results suggested that myeloid *Fbxw7* deficiency led to a marked reduction in the accumulation of pro-inflammatory MPh in colitis microenvironment.

***Fbxw7* deficiency downregulated *Ccl2/Ccl7* in resident macrophages**

The abnormal phagocytosis of invading microbes by resident macrophages could induce excessive inflammation (28). We first confirmed that *Fbxw7* deficiency did not affect the phagocytic function of macrophages by detecting the phagocytosis efficiency of bone marrow-derived macrophages (BMDMs) from *LysM*$^{+}$*Fbxw7*$^{f/f}$ mice or *Fbxw7*$^{f/f}$ littermates (supplementary figure S8A) and did not influence the expression of phagocytosis related genes (*Mfge8, Timd4, Anxa1*) in primary peritoneal or CLP macrophages (supplementary figure S8B). *Fbxw7* deficiency in macrophages also did not impact the survival of macrophages after serum depletion (supplementary figure S8C).

Inflammatory cytokines TNF-α and IL-6 were predominantly produced by inflammatory MPh during colitis. We then examined whether *Fbxw7* deficiency decreases the expression of cytokines (3). ELISA analysis revealed comparable inflammatory

cytokines production (TNF-α, IL-6, IL-10) in *LysM*$^{+}$*Fbxw7*$^{f/f}$ and *Fbxw7*$^{f/f}$ colon tissue 5 days after DSS challenge (figure 5A, supplementary figure S9A), the mRNA expression of cytokine genes in BMDMs from *LysM*$^{+}$*Fbxw7*$^{f/f}$ and *Fbxw7*$^{f/f}$ mice showed no significant difference (supplementary figure S9B). Local inflammation and tissue damage in UC and CD are affected by local expression of specific chemokines within IBD tissues (29), and DSS colitis correlates directly with the CCR2-mediated accumulation of MPh (30). To address the mechanisms involved in the downregulation of intestine inflammation by myeloid deficiency of *Fbxw7*, CX3CR1^{hi} resident macrophages, CX3CR1^{int} pro-inflammatory MPh and Ly6C^{hi} monocytes populations were sorted. CX3CR1^{hi} resident macrophages express significantly higher chemokines than those in CX3CR1^{int} pro-inflammatory MPh (supplementary figure S9C). Then, transcriptome analysis with macrophages from *LysM*$^{+}$*Fbxw7*$^{f/f}$ mice and *Fbxw7*$^{f/f}$ littermates identified the differentially expressed genes and also revealed that the myeloid *Fbxw7* deficiency leads to a significantly decreased expression of various inflammation related genes, among which *Ccl2/7* are the most significant (figure 5B). Decreased expression of the cytokines in *LysM*$^{+}$*Fbxw7*$^{f/f}$ mice tissue at the later phase of colitis (9 days after DSS treatment) (figure 5A) might be the consequence of the substantial decrease of inflammatory MPh infiltration. *LysM*$^{+}$*Fbxw7*$^{f/f}$ mice displayed significantly lower levels of *Ccl2* and *Ccl7* in resident macrophage population compared with *Fbxw7*$^{f/f}$ littermates, whose functions were mainly involved in the recruitment of monocytes (figure 5C). qRT-PCR (supplementary figure S9D-E) and ELISA (figure 5D and supplementary figure S9F) further confirmed that myeloid deficiency of *Fbxw7* resulted in lower levels of CCL2 and CCL7 in macrophages from colitis mice. Moreover, macrophage-depleted *LysM*$^{+}$*Fbxw7*$^{f/f}$ mice and *Fbxw7*$^{f/f}$ littermates showed similar expression level of chemokines CCL2 and CCL7 (Figure 5D). We also observed a significant correlation between *Fbxw7* mRNA levels with *Ccl2* mRNA levels in colonic mucosa sample from patients with ulcerative colitis (UC) collected from GEO database (supplementary figure S9G). Collectively, these results suggested that myeloid *Fbxw7* deficiency decreased the production of *Ccl2/7* in resident macrophages.

Monocyte migration from peripheral blood during infection or inflammation requires CCL2/7 (CCL2 and CCL7)-CCR2 (31), transwell migration assay was utilized to compare the chemo-attractive function of resident macrophages from *LysM*$^{+}$*Fbxw7*$^{f/f}$ mice and *Fbxw7*$^{f/f}$ littermates in vitro (supplementary figure S10A-B). *LysM*$^{+}$*Fbxw7*$^{f/f}$ resident macrophages recruited fewer monocytes than *Fbxw7*$^{f/f}$ littermates in a transwell assay (figure 5E and supplementary figure S10C). Furthermore, CCL2/7 production was decreased in the culture supernatant of CX3CR1^{hi} resident macrophages from *LysM*$^{+}$*Fbxw7*$^{f/f}$ mice compared with those from *Fbxw7*$^{f/f}$ littermates (figure 5F). Compared with resident macrophages, the culture supernatant of pro-inflammatory MPh from both *LysM*$^{+}$*Fbxw7*$^{f/f}$ mice and *Fbxw7*$^{f/f}$ littermates showed the weaker ability to recruiting monocytes (figure 5E and supplementary figure S10C) with lower levels of chemokines (figure 5F). Importantly, neutralization of CCL2/7 abrogated the difference in the monocyte-recruiting ability of *Fbxw7*$^{f/f}$ and *LysM*$^{+}$*Fbxw7*$^{f/f}$ resident macrophages (figure 5G, supplementary figure S10D). This observation suggested that decreased production of CCL2/7 in *LysM*$^{+}$*Fbxw7*$^{f/f}$ resident macrophages contributed to the reduced recruitment of Ly6C^{hi} monocytes. Furthermore, anti-CCL2/7 antibodies decreased the number of inflammatory MPh infiltrated in the colon of both *Fbxw7*$^{f/f}$ and *LysM*$^{+}$*Fbxw7*$^{f/f}$ mice (supplementary figure S11A-B) and abrogated the alleviated colitis phenotype of *LysM*$^{+}$*Fbxw7*$^{f/f}$ mice (figure 5H-I, supplementary figure S11C-D). Moreover, we adoptively transferred mixed *Fbxw7*$^{f/f}$ and *LysM*$^{+}$*Fbxw7*$^{f/f}$ monocytes into *Fbxw7*$^{f/f}$ or *LysM*$^{+}$*Fbxw7*$^{f/f}$ recipient mice (supplementary figure S11E). Flow cytometry analysis showed that *LysM*$^{+}$*Fbxw7*$^{f/f}$ recipient mice failure to recruit monocytes to their inflamed colon when compared with *Fbxw7*$^{f/f}$ littermates (figure 5J). Collectively, these data further support that *Fbxw7* deficiency decreased the expression of CCL2/7 in resident macrophages and thereby reducing the accumulation of pro-inflammatory MPh during the progress of colitis.

FBXW7 interacts with EZH2

To identify the mechanisms regulating CCL2/7 production in colon resident macrophages, the activation of NF-κB and HIF-1α (32,33) pathways were detected during LPS-induced

response. There is no potent difference in these signaling pathways between *Fbxw7*$^{f/f}$ and *LysM*$^{+}$*Fbxw7*$^{f/f}$ BMDMs after LPS stimulation (figure 6A-B). These results raise the possibility of epigenetic regulation of *Ccl2/7* gene in response to inflammatory stimuli. We next detected the changes of histone modifications. The modification of H3K27me3 was significantly increased in *LysM*$^{+}$*Fbxw7*$^{f/f}$ BMDMs compared with *Fbxw7*$^{f/f}$ BMDMs after LPS stimulation (figure 6C). EZH2 was found to be an important enzyme for H3K27me3, the decreased protein of EZH2 was observed in BMDMs after challenged with LPS (supplementary figure S12A). The expression of EZH2 was also decreased in CD11b^{+} macrophages from CLP of IBD mice compared with healthy controls (supplementary figure S12B). We speculated that EZH2 protein expression negatively correlates with FBXW7 level in CLP macrophages. Increased EZH2 protein was found in *Fbxw7* deficient BMDMs than *Fbxw7*$^{f/f}$ BMDMs upon LPS stimulation (figure 6D). Furthermore, the interaction of endogenous EZH2 and FBXW7 in BMDMs was increased after LPS challenge (figure 6E). Consistently, FBXW7 co-localized with EZH2 upon LPS stimulation in BMDMs (figure 6F).

FBXW7 recognizes and binds to the substrates through a stretch of eight WD40 repeat domain (34), the binding consensus motif (T/S)PXX(S/T/D/E) has been identified in several FBXW7 substrates, including c-Myc, cyclin E1 and c-Jun (35-37). Protein motif analysis showed that two domains in EZH2 protein sequence might be the FBXW7 binding motif (figure 6G). To determine whether those amino acid sequences were required for FBXW7 recognition and ubiquitination, we constructed three mutants of EZH2 in which serine at position 261, 265 and 367, 371 were replaced with glycine. The results showed that mutant EZH2 (261, 265A) and mutant EZH2 (367, 371A) bound to FBXW7 less efficiently than EZH2, mutant EZH2 (261, 265 and 367, 371, 4A) could not bound FBXW7 (figure 6H). These results strongly suggest that the serine at position 261, 265, 367 and 371 of EZH2 were critical for its interaction with FBXW7.

FBXW7 mediates the degradation and ubiquitination of EZH2

To address whether EZH2 was the target of FBXW7 in macrophages, we observed that there was no significant difference in *Ezh2* mRNA expression upon LPS stimulation between *Fbxw7*$^{f/f}$ and *LysM*$^{+}$*Fbxw7*$^{f/f}$ BMDMs (supplementary figure S12C), but the decreased protein expression of EZH2 after LPS stimulation (supplementary figure S12A) was completely blocked by the proteasome inhibitor MG132 (figure 7A). The cycloheximide chase assay showed that FBXW7 deficiency extended the half-life of endogenous EZH2 protein in BMDMs (figure 7B-C). These data indicated that FBXW7 might induce EZH2 degradation through proteasome. The exogenous expressed EZH2 was degraded by overexpressed FBXW7 in HEK293 cells, which was also abrogated by MG132 (figure 7D). However, FBXW7 could not decrease the expression of mutant Ezh2 (4A) (figure 7E). Collectively, these results indicated that EZH2 could be degraded by FBXW7 via ubiquitin-proteasome system. To investigate whether FBXW7 functions as an E3 ubiquitin ligase of EZH2, we observed that the ubiquitination of EZH2 mediated by FBXW7 through a dose-dependent way (figure 7F). FBXW7 could induce K48-linked polyubiquitination on EZH2 (figure 7G). Furthermore, FBXW7 deficiency in macrophages almost canceled K48-linked polyubiquitination on endogenous EZH2 compared with wild type macrophages (figure 7H). Together, these data demonstrate that FBXW7 promotes K48-linked polyubiquitination and proteasome degradation of EZH2 in macrophages.

EZH2 inhibits macrophage *Ccl2/7* expression by H3K27me3 modification

EZH2 has been revealed to be recruited to the proximal promoter of *Ccl2* gene in a clock gene BMAL1 dependent manner (38). We hypothesized that FBXW7 increases chemokine CCL2/7 expression by decreasing the protein level of EZH2. *Ezh2* was knocked down by Ezh2 siRNA (siEzh2) in BMDMs, siEzh2 reduced expression of EZH2 and H3K27me3 level as compared with siNC (figure 8A). Knockdown of *Ezh2* enhanced *Ccl2/7* mRNA expression in BMDMs and mitigated the difference of LPS-induced CCL2/7 expression between *Fbxw7*$^{f/f}$ and *LysM*$^{+}$*Fbxw7*$^{f/f}$ BMDMs (figure 8B). To test the direct effect of EZH2-associated H3K27me3 on expression of *CCL2/7*, BMDMs were treated with GSK126, an EZH2 specific competitive inhibitor compound (39), this inhibitor induced

loss of EZH2-associated H3K27me3 without any change in EZH2 protein abundance (figure 8C), GSK126 treatment also showed the consistent result with siEzh2 (figure 8D). These data indicate that FBXW7 regulates CCL2/7 expression via EZH2 associated H3K27me3. Chromatin immunoprecipitation (ChIP) assay revealed higher H3K27me3 modification in the proximal promoter areas of *Ccl2/7* gene in $LysM^{+}Fbxw7^{f/f}$ BMDMs than those in $Fbxw7^{f/f}$ BMDMs (figure 8E). These data suggest that FBXW7 promotes *Ccl2/7* chemokine expression by inhibiting EZH2-dependent methylation of H3K27 at the promoters of *Ccl2/7* genes.

Reducing the expression of *Fbxw7* alleviates colitis

The results above demonstrated that FBXW7 expression was positively correlated with the severity of colitis, underscoring the therapeutic potential of FBXW7. To further explore the therapeutic importance of FBXW7 in colitis, recombinant adeno-associated virus (AAV-shFbxw7 or AAV-shNC vector as a control) was injected into proximal bowel in mice. High-efficiency transduction of GFP-pAAV-shFbxw7 vector was verified in C57BL/6 mice by immunofluorescence (supplementary figure S13A) and qRT-PCR (supplementary figure S13B). AAV-shFbxw7 treatment could decrease the mucosa ulcerations in *Il10* KO colitis mice (figure 9A-B). In DSS induced colitis model, AAV-shFbxw7 treated C57BL/6 mice exhibited a lower loss of body weight, lower DAI (figure 9C), alleviated colon phenotype and shortening (figure 9D-E), when compared with AAV-shNC mice. Moreover, AAV-shFbxw7 treated mice showed significantly decreased *Ccl2/7* expression in colon tissues, while not significant change in expression of Ccr2 and Cx3cl1 (figure 9F). Also, AAV-shFbxw7 treatment significantly improved colitis mice survival (figure 9G) compared with AAV-shNC mice. Altogether, these results suggest that AAV-mediated colonic *Fbxw7* silence protected colitis mice against inflammation development and disease progression by downregulating *Ccl2/7*.

Discussion

E3 ubiquitin ligases FBXW7 is mutated in ~10% of human colon cancers, it acts as a tumor suppressor in several tissues, targets multiple transcriptional activators and proto-oncogenes for ubiquitin-mediated degradation (40). However, the role of FBXW7 in inflammation and immune response remains unknown. In this study, we revealed a novel mechanism for mediating IBD progression that FBXW7 promotes *Ccl2/7* expression through degrading EZH2 in CX3CR1^{hi} resident macrophages, which results in increased recruitment of CXCR1^{int} MPh and amplification of intestine inflammation. Our work provides new insights into clarifying the molecular and cellular networks of the intestine inflammatory microenvironment.

A constant balance between the resident macrophages and inflammatory MPh is critical for maintaining the status quo in a healthy gut and ensuring protective immunity when required. Interestingly, we noticed a more marked reduction of CD11b^{+}CX3CR1^{hi} resident macrophages compared with CD11b^{+}CX3CR1^{int} inflammatory MPh after liposome injection. This preferential ability may be due to the higher phagocytic activity of CD11b^{+}CX3CR1^{hi} resident macrophages (41), which are key players in capturing and destroying invading pathogens, as well as clearing apoptotic or senescent cells due to their high phagocytic capacity. The findings suggested that increased susceptibility of DSS-induced colitis in both *Fbxw7*$^{f/f}$ and *LysM*$^{+}$*Fbxw7*$^{f/f}$ mice after liposome treatment is related to the depletion of their resident macrophages in the colon. Furthermore, it is highly probable that the disappearance of the severity difference between *Fbxw7*$^{f/f}$ and *LysM*$^{+}$*Fbxw7*$^{f/f}$ mice during colitis is due to the elimination of macrophages.

Altered profiles of inflammatory molecules and inflammation related signaling pathway, including cytokines, chemokines, inflammasomes, antimicrobial peptides and neuropeptides are all involved in the pathogenesis of Crohn's disease and ulcerative colitis (3). The degree of local inflammation and tissue damage in UC and CD is dependent on local expression of specific chemokines within IBD tissues. Genome-wide association studies have pointed several IBD susceptibility loci that contain genes that encode proteins involved in chemokine signaling, including CC-chemokine receptor 6

(*CCR6*), *CCL2* and *CCL13*. A recent study has reported that treatment of intestinal crypts with supernatants of commensal-specific T cells from CD patients induced higher protein secretion of chemokines CXCL8 and CXCL1, and prompted a predominant neutrophil and Th17 recruitment to the intestinal epithelium (42). The expression of *Il17C* mRNA has been identified to correlate with *CCL20* in the inflamed colon of IBD patients (43). We found that upregulated *Fbxw7* in the inflamed intestine in macrophages promotes CCL2/CCL7 production to facilitate the progression of colitis by potently recruiting pro-inflammatory MPh. On the other hand, protective role of *Fbxw7* in intestinal epithelium during acute intestinal inflammation has also been reported, deletion of *Fbxw7* in the intestinal epithelium promotes colitis induced by DSS through activating the NF-κB signaling (44). Their findings and our study revealed the differential function of *Fbxw7* in intestinal epithelium and myeloid cells within the intestine microenvironment.

During inflammation, the epigenetic mechanisms have been known recently to determine the unique tissue specific identity and function of macrophages (45,46). Trimethylation of H3k4 on cytokine gene promoters was shown to be induced in active M1 macrophages in response to TLR stimulation, leading to chromatin remodeling and inflammatory gene expression (47). IFNγ-dependent histone acetylation regulation instructs the development of the colitogenic monocyte and macrophage lineage in vivo during inflammation, suggesting a new insight of how macrophages gain colitogenic properties during the development of colitis (48). Demethylase KDM6A has been reported to promote cytokines IL-6 and IFN-β transcription in primary macrophages during innate response through demethylating H3K27me3 at the promoters of *Il6* and *Ifnb* (49). A selective H3K27 demethylase inhibitor was also demonstrated to reduce LPS-induced pro-inflammatory cytokine production by human primary macrophages (50). EZH2 acting as a catalytic subunit of PRC2 is critical in mediating the formation of H3K27me3, which is associated with transcriptional gene suppression (51). Ezh2 deficiency has been shown to affect TNF-α signaling, and promote the inflammatory response in intestinal epithelial cells in colitis (52). We provide evidence that the threonine at position 261 and 367 of EZH2 was essential for its interaction with FBXW7, which mediates the function of FBXW7 in

reducing EZH2 expression in resident macrophages upon DSS challenge. The relationship between FBXW7 and epigenetic modifiers has been reported in tumorigenesis (53), but it remains largely unknown in inflammation. We have demonstrated that CCL2/7 produced by resident macrophages of *LysM*$^{+}$*Fbxw7*$^{f/f}$ mice were lower than those in *Fbxw7*$^{f/f}$ littermates, a selective inhibitor of H3K27me3 in macrophages exhibit the effect of promoting *Ccl2/7* expression.

In summary, we demonstrated the critical role of FBXW7 in regulating colitis by inducing *Ccl2* and *Ccl7* in resident macrophages and promoting the accumulation of proinflammatory MPh. FBXW7/EZH2/CCL2/7 is an important pathway in shaping the status and activity of colonic resident macrophages and inflammatory MPh in colitis condition. Our results provide the possibility for FBXW7 to be a predictive marker of IBD severity and a potential target for IBD treatment since the siRNA of *Fbxw7* showed a significant therapeutic effect in colitis mouse model.

Methods

Mice and reagents. Fbxw7$^{f/f}$ mice (C57BL/6J) were obtained from Jackson Laboratories. LysM-Cre mice C57BL/6J were kindly provided by Dr. Ximei Wu, Zhejiang University School of Medicine, Hangzhou, P. R. China. *Il10$^{-/-}$* KO mice were kindly provided by Dr. Yanmei Han, National Key Laboratory of Medical Immunology & Institute of Immunology, Second Military Medical University, Shanghai, P. R. China. All mice were bred at the Zhejiang University Laboratory Animal Center under specific pathogen-free conditions. C57BL/6 mice were purchased from Model Animal Research Center of Nanjing University (Nanjing, P. R. China).

Mice were born and bred at the same facility, they were kept at the same rack of an animal room, maintained under specific pathogen-free conditions with controlled temperature (22°C) and photoperiod (12/12-hlight/dark cycle), allowing unrestricted access to standard mouse chow and water, except for some special experiments that were specially explained. The cohousing experiments were performed with 3-week-old weaned *Fbxw7$^{f/f}$* mice randomly cohoused with age-matched *LysM^{+} Fbxw7$^{f/f}$* mice at a 1:1 ratio for 7 weeks prior to DSS colitis induction while mice remained cohoused.

Antibodies to the HA tag (sc-805), Myc tag (sc-40; sc-789), Flag tag (sc-807), GAPDH (sc-130619), ubiquitin (sc-271289) were from Santa Cruz. Antibodies specific for p-p65 (3033), p65 (8242), Ezh2 (3147), HIF-1α (36169) were from Cell Signaling Technology. Lys48-specific linked polyubiquitin antibody (05-1307) was from Millipore. Antibodies to the FBXW7 were from Abcam (ab12292) and Thermo Fisher (40-1500). Antibodies to the H3K36me3 (ab9050), H3K9me3 (ab8898), H3K4me3 (ab8580), H3K27me3 (ab6002) and H3 (ab1791) were from Abcam. MG132 (M8699), CHX (C4859) and Flag-M2 Magnetic Beads (M8823) were from Sigma-Aldrich. ELISA kits for mouse IL-6 (BMS603-2), TNF-α (BMS607-3), CCL2 (BMS6005) and CCL7 (BMS6006INST) were from eBioscience.

Human peripheral blood samples. A total of 68 peripheral blood samples were collected from IBD patients hospitalized in Sir Run Run Shaw Hospital, Zhejiang University School of Medicine, China, from 11 May 2017 to 1 August 2017, and 50 healthy adults as a

control group. The diagnosis and severity evaluation of IBD were according to the Expert consensus document on the diagnosis and treatment of IBD (2017). The severity of CD disease was determined according to Best CDAI calculator (54). The severity of UC disease was determined by Mayo Score by composite indices (55). The basic information from all of the patients, including age and sex, was summarized in supplementary Table 1.

Monocytes were isolated using a human monocyte isolation kit (Haoyang Biological Technology Co., Tianjin, P. R. China) according to the manufacturer's recommendations.

Randomization method. The following covariates of mice were controlled: age, gender, littermate status, adult mice (8-10 week of age) of male and its littermates were used. Under such conditions, mice were randomly assigned to experimental groups. For studies using media collected from stimulated cells or tissues was randomly allocated to ELISA plate wells prior to measurement. Random fields were analyzed in confocal images, H&E images and immunohistochemical images.

Fecal microbiome analysis. *LysM*$^{+}$ *Fbxw7*$^{f/f}$ and *Fbxw7*$^{f/f}$ littermates (8 to 10-week-old male or female C57BL/6J mice) were fed in different cages. They were kept in the same environment with other experimental mice. Fresh formed feces were collected from the cage and weighted. Bacterial DNA was extracted from the stool using a QIAamp Fast DNA Stool Mini Kit (Qiagen). DNA concentration and purity were monitored on 1% agarose gels, after which DNA was diluted to 1 ng/μl using sterile water.

Amplicon Generation, PCR products mixing and purification, Library preparation and sequencing of the 16S rDNA gene were performed to determine the bacterial composition and diversity by Novogene Bioinformatics Technology Co., Ltd, through using IonS5^{TM}XL 16S rDNA amplicon sequencing. Sequencing libraries were generated using Ion Plus Fragment Library Kit 48 rxns (Thermofisher) following manufacturer's recommendations. Data analysis was also provided by Novogene Bioinformatics Technology Co., Ltd according to the previous literature (56,57). Statistical analysis of sequence data was

performed by Uparse software (Uparse v7.0.100, http://drive5.com/uparse/) (58). Sequences with ≥97% similarity were assigned to the same OTUs.

Cell culture. HEK293T cells (ATCC, CRL-11268) were maintained in DMEM medium, Thioglycolate (BD, 3190383, Merck, 1.08191.0500)-elicited mouse peritoneal macrophages were cultured in RPMI-1640 medium with 10% (vol/vol) FCS. Bone marrow derived macrophages (BMDMs) were generated from the bone marrow from femurs and tibias of 6- to 8-week-old mice (25).

Induction of colitis. 8 to 10 week-old *LysM*$^{+}$*Fbxw7*$^{f/f}$ C57BL/6 mice and *Fbxw7*$^{f/f}$ littermates were studied using TNBS or DSS-induced colitis models as described (59). Mice were treated with 3% DSS (MP Biomedical) in drinking water (w/v) for 7 days and followed by 2 days water before sacrificed. In recovery experiment, *LysM*$^{+}$*Fbxw7*$^{f/f}$ and *Fbxw7*$^{f/f}$ littermates treated with 7 days DSS, followed by 13 days recovery, control mice were treated with water. In a survival experiment, the mice were fed with 4% DSS for 7 days and followed by regular drinking water until the end of the study.

Overnight-fasted mice were intrarectal injected 100 mg/kg 2,6,4-trinitrobenzene sulfonic acid (TNBS, Sigma-Aldrich) in 50% ethanol, with 50% ethanol treatment as a control, *LysM*$^{+}$*Fbxw7*$^{f/f}$ and *Fbxw7*$^{f/f}$ littermates were sacrificed 5 days after TNBS treatment.

Il10$^{-/-}$ mice spontaneously develop a chronic IBD under specific pathogen-free conditions in our animal facility. The phenotypes of chronic enterocolitis were more evident when *Il10* $^{-/-}$ mice were 12 weeks or older.

Analysis of colon explant cultures and ELISA. The colons of mice were flushed with PBS containing 30% antibiotics, and open along a longitudinal axis. Then almost 3 mm^2 pieces of tissue was obtained from the distal colon and incubated for 24 hours in RPMI supplemented with 10% fetal calf serum and 20% antibiotics (one punch biopsy per 100 ml medium). Supernatants were collected and kept frozen until assessed. The CCL2 and

CCL7 levels in the supernatant were detected by conventional double-sandwich ELISA (BD Biosciences).

Flow Cytometry. The following fluorochrome labelled monoclonal antibodies and staining reagents were used according to manufacturer's protocols: lamina propria cells were stained with anti-CD11b-FITC (BioLegend, 101217), anti-Ly6C-FITC (BioLegend, 128005), anti-Gr-1-FITC (BioLegend, 108417), anti-CD11b-PE (BioLegend, 101208), anti-CX3CR1-PE (BioLegend, 149006), anti-CD11C-APC (BioLegend, 117310), anti-F4/80-FITC (BioLegend, 123120), anti-Ly6G-FITC (BioLegend, 127605), anti-CD45.2-APC (eBioscience,104). anti-Ly6C-percp cy5.5, FVD (Zombie VioletTM Fixable Viability Kit, BioLegend, 423114), anti-F4/80-CF594 (BioLegend, 123131), anti-CD103-BV605 (BD, 740355), anti-Ezh2-FITC (BD, 562479), hCdc4 Antibody (Thermo, 40-1500). The cells were analyzed with NovoCyteTM flow cytometer (ACEA), BD Fortessa or sorted with a FACSAria machine (BD). Flow cytometry analysis was done with the FlowJo software.

Gene expression analysis. Total RNA was extracted from cells using TRIzol reagent (Takara) according to the manufacturer's directions. Subsequently, single-strand cDNA synthesis was performed using the reverse transcription kit (Toyobo), in the DSS-induced colitis model, RNA reverse transcription was performed as previously described (60). Total cDNA of macrophages and monocytes sorted from mice colon were extracted using Single Cell Sequence Specific Amplification Kit (Vazyme). qRT-PCR was performed using the SYBR Green master Rox (Roche) on CFX-96 (Bio-Rad) or 480II (Roche) Real-Time PCR System and β-actin was used as housekeeping gene. The primer sequences are listed in supplementary table 2.

Monocyte transfer experiment. Briefly, recipient mice underwent sub-lethal dose of γ-ray irradiation (8 Gly) to induce damage of the bone marrow cells at day 3 or 7 after DSS challenge and 6 hours post-irradiation, *LysM*$^{+}$*Fbxw7*$^{f/f}$ (KO) and *Fbxw7*$^{f/f}$ littermates (WT)

recipients were received 100 μl fresh WT and KO mixed monocytes, labeled by cell proliferation Dye eFluor 450 (eBioscience, 65-0842-90) and 670 (eBioscience, 65-0840-85) with the concentration of 1×10^7/ml respectively, which are WT+KO→WT and WT+KO→KO groups. Ly6C^{hi} monocytes were sorted to high purity (>95%), 1 day after monocytes transfer, mice's colonic lamina propria (CLP) were collected and analyzed by flow cytometry.

Migration assay. 1×10^4 sorted splenic Ly6C^{hi} monocytes from *Fbxw7$^{f/f}$* or *LysM$^+$Fbxw7$^{f/f}$* mice were added into the upper compartment of transwell chambers (24-well plate, 8-mm pores, BD Biosciences) in 100 μl of serum-free medium. 5×10^5 sorted CX3CR1^{hi} resident or CX3CR1^{int} pro-inflammatory MPh from CLP of *Fbxw7$^{f/f}$* or *LysM$^+$Fbxw7$^{f/f}$* colitis mice were cultured in 600 μL RPMI 1640 serum-free medium, after 24 hours, the culture supernatant was harvested and added into the lower chamber of the transwell plate as a chemotactic stimulus. In some conditions, CCL2 (R&D Systems, AF-479-NA) and CCL7 (R&D Systems, AF-456-NA) antibody were added into the conditioned medium in lower chamber 2 hours before incubation. After 24 hours inoculation at 5% CO_2, 37°C, the cells dropped into lower chamber were counted by cytometry and cells that cling to the bottom side of polycarbonate membrane were fixed by 10% formalin and stained with DAPI.

For migration assay in vivo, mice were administered of anti-CCL2/7-Ab (R&D Systems, AF-479-NA and AF-456-NA) or rat IgG2a isotype control mAb (Biolegend, RTK2758) diluted in sterile PBS by intraperitoneal injection every 48 hours on days -1, 1, 3 and 5 during DSS treatment.

Phagocytosis assay. Fluorescein conjugate Escherichia coli (K-12 strain) BioParticles™ (Molecular Probes, E2861, FITC-labeled heat-killed E. coli) were diluted in serum media and incubated for 30 min followed by 2 time washes in PBS, FITC-labeled heat-killed E. coli was added in RPMI-1640 medium with 10% FCS and incubated with cells for 1 hour in a humidified atmosphere with 5% CO_2 at 4°C or 37°C, then cells were washed two times

with PBS before trypsinization，then washed one time with trypan blue and analyzed by flow cytometry.

Depletion of macrophages. Macrophages were depleted using clodronate-containing liposomes (CLs; ClodronateLiposomes.org, Amsterdam, Netherlands) consulted previously (61). In brief, mice were anesthetized, and CLs was injected via tail vein (100 μl) and intraperitoneal (100 μl) into mice on days -1, 1, 3, and 5 during DSS treatment. Liposome-encapsulated PBS was not used as a negative control, because the uptake of these liposomes by colonic macrophages was shown to result in a partial reduction of macrophages (62). Controls included i.p. injections of 200 μl PBS.

Preparation of mouse neutrophils from peripheral blood. Mouse blood (350 ± 50 μl per animal) was collected by tail bleeding from mice into Hanks' balanced saline solution (HBSS)-EDTA (HBSS without calcium, magnesium, phenol red, and sodium bicarbonate; pH=7.2, 15 mM EDTA, bovine serum albumin (BSA), 1%). Neutrophils was isolated by using Percoll-based density gradient centrifugation (63), 350,000 ± 40,000 cells were obtained per mouse, 97% neutrophils.

Neutrophil depletion. Mice were administered 400 μg of anti-Ly6G mAb (Biolegend, 1A8) or rat IgG2a isotype control mAb (Biolegend, RTK2758) diluted in sterile PBS by intraperitoneal injection every 48 h on days -1, 1, 3, and 5 during DSS treatment. For confirmation of depletion during colitis experiments, colons from anti-Ly6G treated mouse and isotype treated mouse in health or colitis were harvested from each independent experiment and analyzed by flow cytometry for a reduction in $CD45^+CD11b^+Gr\text{-}1^+$ cells.

Immunohistochemical and immunofluorescence staining. Colon tissues were fixed in 4% formalin, immunohistochemical and immunofluorescence staining was performed for human and mouse colonic sections by the Histomorphology Platform of Zhejiang

University, with the standard protocol performed according to the manufacturer's instructions. Human colonic specimens were scored using Constantine's protocol (64), under high magnification, integrated staining intensity and the percentage of positive cells were scored.

Colitis analysis. Colons were collected immediately after mice sacrifice, the entire colon (from the cecum to anus) was removed and measured, colonic length was reported as described previously (65). Distal colon was removed, fixed in 10% formalin, then embedded the tissue sections with paraffin and stained with H&E, for light-microscopic examination to assess colon injury and inflammation, the degree of colitis was scored without any prior knowledge of experimental procedures as follows (66), including degree of epithelial regeneration (scale of 0-3), distortion/branching (scale of 0-3), inflammation (scale of 0-3) and crypt damage (0-4), percentage of area involved by inflammation (0-4) and crypt damage (0-4), and depth of inflammation (0-3), was applied. The total score is 0 point (no colitis) to 24 points (severe colitis).

In TNBS induced colitis, disease activity index (DAI) (scale of 0-4) was monitored daily and used to assess the severity of colitis based on weight loss, stool bleeding and stool consistency according to the methods described previously (67).

Plasmid constructs and transfection. Recombinant vectors encoding mouse *Ezh2* were created by PCR-based amplification of complementary DNA of mouse bone marrow cells, followed by subcloning into the Pcmv-Tag2B eukaryotic expression vector (Invitrogen) as described. All constructs were confirmed by DNA sequencing. The plasmids were transfected into HEK293T cells with JetPrime (Polyplus). Primary macrophages transfected with siRNA through the use of INTERFERin reagent (Polyplus) according to the standard protocol. BMDMs were transfected with siRNA through the use of INTERFERin reagent (Polyplus) according to the standard protocol. *Ezh2* siRNA sequences were 5'-GCACAAGTCATCCCGTTAA-3', 5'-GCAACACCCAACACATATA-3' and 5'-GCAAATTCTCGGTGTCAAA-3' from Gene Pharma. *Fbxw7* siRNA sequences

were 5'-ACCTTCTCTGGAGAGAGAAATGC-3', 5'-GTGTGGAATGCTGAAACTGGAGA-3' and 5'-CACAAAGCTGGTGTGTGCA-3' from Life Technology.

Immunoprecipitation, immunoblot analysis. SDS-PAGE and immunoblot analysis were performed as described previously (25). BMDMs were immunoprecipitated using anti-FBXW7 plus protein A/G agarose. The proteins were then separated using SDS-PAGE and subjected to immunoblot analysis with anti-EZH2 or anti-FBXW7 antibodies.

Chromatin Immunoprecipitation (ChIP) Analysis. ChIP analysis was performed as described (68) with H3K27me3 (ab6002) and the process was performed according to the manufacturer's instructions of the ChIP assay kit (CST). Fold enrichment was quantified using qRT-PCR and calculated as a percentage of input chromatin (% input).

RNA sequencing. Total RNAs of bone marrow derived macrophages (BMDMs) (1×10^6) were extracted by the manual of TRIzol ® (Takara). Preparation of library and sequencing of transcriptome were carried out using Illumina HiSeq × Ten (Novogene Bioinformatics Technology Co., Ltd., Beijing, P. R. China). The mapping of 100-bp paired-end reads to genes was undertaken using HTSeq v0.6.0 software, while fragments per kilobase of transcript per million fragments mapped (FPKM) were also analyzed. RNA sequencing data are available in the Gene Expression Omnibus repository under accession number GSE125242.

pAAV-EGFP Administration. Mice were fasted overnight, pretreated with 20 mM N-acetyl-L-cysteine (NAC) (Sigma-Aldrich, St. Louis, MO) as described above (69), and anesthetized with chloral hydrate through intraperitoneal injection. The colon was washed with an intrarectal injection of 100 μl of 20 mM NAC using stainless steel straight round-tip microsyringe and allowed to drain for 15 min, and this step was repeated twice. After that, mice were reanesthetized and 5×10^{10} physical particles of pAAV-EGFP in 100 μl of PBS

were given by enema, tail vein injection was given every week until 21 days. The transgene plasmids we used were p-AAV-CMV-EGFP and p-AAV-shFbxw7 (U6-shNC/shFbxw7-mir30arm), generated by Shanghai SunBio Medical Biotechnology Co.

Statistics. Statistical analysis was performed with GraphPad Prism software. All data are expressed as the mean ± SEM or SD. All experiments are repeated at least three times independently. Statistical significance between two experimental groups was determined with unpaired two-tailed Student's *t* test. Differences with a p-value of <0.05 were defined as statistically significant. Three or more groups were compared based on an analysis of variance test. The multiple comparisons between variables were assessed by one-way ANOVA with Tukey's multiple comparisons test. For mice survival study, Kaplan-Meier survival curves were generated and log-rank test (Mantel-Cox) was used for statistical significance.

Study approval. The patients' consent, as well as ethics approval for the use of human samples, was approved by the Medical Ethics Committee of Zhejiang University School of Medicine before harvesting human tissue and blood samples. The animal research used the protocol that has been approved by the Medical Experimental Animal Care Commission of Zhejiang University.

Author contributions

Q. Wang, L. Lai and J. He designed the research. J. He, Y. Song, P. Gao, Y. Liu, Y. Xue, X. Tu, T. Pan, Z. Jiang and L. Lai performed experiments and acquisition, analysis of data. P. Xiao and Q. Cao provided clinical specimens. J. He, L. Lai and Q. Wang wrote the manuscript. X. Cao supervised the study. All authors have read and approved the final manuscript.

Acknowledgments

This work was supported by grants from the National Natural Science Foundation of China (81771699, 31870907, 81571524), National Program on Key Basic Research Project (2014CB542101), and Natural Science Foundation of Zhejiang Province (Z19H100001).

Disclosure of potential conflicts of interest

The authors have declared that no conflict of interest exists.

References

1. de Souza HS, Fiocchi C. Immunopathogenesis of IBD: current state of the art. *Nature reviews. Gastroenterology & hepatology.* 2016;13(1):13-27.
2. Kostic AD, Xavier RJ, Gevers D. The microbiome in inflammatory bowel disease: current status and the future ahead. *Gastroenterology.* 2014;146(6):1489-1499.
3. Neurath MF. Cytokines in inflammatory bowel disease. *Nature reviews. Immunology.* 2014;14(5):329-342.
4. Bain CC, Schridde A. Origin, Differentiation, and Function of Intestinal Macrophages. *Frontiers in immunology.* 2018;9:2733.
5. Mosser DM, Edwards JP. Exploring the full spectrum of macrophage activation. *Nature reviews. Immunology.* 2008;8(12):958-969.
6. Strober W, Fuss IJ. Proinflammatory cytokines in the pathogenesis of inflammatory bowel diseases. *Gastroenterology.* 2011;140(6):1756-1767.
7. Bain CC, et al. Resident and pro-inflammatory macrophages in the colon represent alternative context-dependent fates of the same Ly6Chi monocyte precursors. *Mucosal immunology.* 2013;6(3):498-510.
8. Joeris T, Muller-Luda K, Agace WW, Mowat AM. Diversity and functions of intestinal mononuclear phagocytes. *Mucosal immunology.* 2017;10(4):845-864.
9. Smythies LE, et al. Human intestinal macrophages display profound inflammatory anergy despite avid phagocytic and bacteriocidal activity. *The Journal of clinical investigation.* 2005;115(1):66-75.
10. Zigmond E, et al. Ly6C hi monocytes in the inflamed colon give rise to proinflammatory effector cells and migratory antigen-presenting cells. *Immunity.* 2012;37(6):1076-1090.
11. Grainger JR, Konkel JE, Zangerle-Murray T, Shaw TN. Macrophages in gastrointestinal homeostasis and inflammation. *Pflugers Archiv : European journal of physiology.* 2017;469(3-4):527-539.
12. Bain CC, Mowat AM. Macrophages in intestinal homeostasis and inflammation. *Immunological reviews.* 2014;260(1):102-117.
13. Zigmond E, Jung S. Intestinal macrophages: well educated exceptions from the rule. *Trends in immunology.* 2013;34(4):162-168.
14. Asano K, et al. Intestinal CD169(+) macrophages initiate mucosal inflammation by secreting CCL8 that recruits inflammatory monocytes. *Nature communications.* 2015;6:7802.
15. Lieber S, et al. Prognosis of ovarian cancer is associated with effector memory CD8(+) T cell accumulation in ascites, CXCL9 levels and activation-triggered signal transduction in T cells. *Oncoimmunology.* 2018;7(5):e1424672.
16. Wunderlich CM, et al. Obesity exacerbates colitis-associated cancer via IL-6-regulated macrophage polarisation and CCL-20/CCR-6-mediated lymphocyte recruitment. *Nature communications.* 2018;9(1):1646.
17. Gaujoux R, et al. Cell-centred meta-analysis reveals baseline predictors of anti-TNFalpha non-response in biopsy and blood of patients with IBD. *Gut.* 2018.
18. Kochumon S, et al. Palmitate Activates CCL4 Expression in Human Monocytic Cells via TLR4/MyD88 Dependent Activation of NF-kappaB/MAPK/ PI3K Signaling Systems. *Cellular physiology and biochemistry : international journal of experimental cellular physiology, biochemistry, and pharmacology.* 2018;46(3):953-964.

19. Sans M, et al. Enhanced recruitment of CX3CR1+ T cells by mucosal endothelial cell-derived fractalkine in inflammatory bowel disease. *Gastroenterology.* 2007;132(1):139-153.
20. Taki M, et al. Snail promotes ovarian cancer progression by recruiting myeloid-derived suppressor cells via CXCR2 ligand upregulation. *Nature communications.* 2018;9(1):1685.
21. Welcker M, Clurman BE. FBW7 ubiquitin ligase: a tumour suppressor at the crossroads of cell division, growth and differentiation. *Nature reviews. Cancer.* 2008;8(2):83-93.
22. Onoyama I, et al. Fbxw7 regulates lipid metabolism and cell fate decisions in the mouse liver. *The Journal of clinical investigation.* 2011;121(1):342-354.
23. Yumimoto K, Matsumoto M, Onoyama I, Imaizumi K, Nakayama KI. F-box and WD repeat domain-containing-7 (Fbxw7) protein targets endoplasmic reticulum-anchored osteogenic and chondrogenic transcriptional factors for degradation. *The Journal of biological chemistry.* 2013;288(40):28488-28502.
24. Ekholm-Reed S, Goldberg MS, Schlossmacher MG, Reed SI. Parkin-dependent degradation of the F-box protein Fbw7beta promotes neuronal survival in response to oxidative stress by stabilizing Mcl-1. *Molecular and cellular biology.* 2013;33(18):3627-3643.
25. Song Y, et al. E3 ligase FBXW7 is critical for RIG-I stabilization during antiviral responses. *Nature communications.* 2017;8:14654.
26. Arranz A, et al. Akt1 and Akt2 protein kinases differentially contribute to macrophage polarization. *Proceedings of the National Academy of Sciences of the United States of America.* 2012;109(24):9517-9522.
27. Nishikawa K, et al. Interleukin-17 induces an atypical M2-like macrophage subpopulation that regulates intestinal inflammation. *PloS one.* 2014;9(9):e108494.
28. Geissmann F, et al. Development of monocytes, macrophages, and dendritic cells. *Science.* 2010;327(5966):656-661.
29. Banks C, Bateman A, Payne R, Johnson P, Sheron N. Chemokine expression in IBD. Mucosal chemokine expression is unselectively increased in both ulcerative colitis and Crohn's disease. *The Journal of pathology.* 2003;199(1):28-35.
30. Platt AM, Bain CC, Bordon Y, Sester DP, Mowat AM. An independent subset of TLR expressing CCR2-dependent macrophages promotes colonic inflammation. *Journal of immunology.* 2010;184(12):6843-6854.
31. Serbina NV, Pamer EG. Monocyte emigration from bone marrow during bacterial infection requires signals mediated by chemokine receptor CCR2. *Nature immunology.* 2006;7(3):311-317.
32. Hoesel B, Schmid JA. The complexity of NF-kappaB signaling in inflammation and cancer. *Molecular cancer.* 2013;12:86.
33. Storti P, et al. Hypoxia-inducible factor (HIF)-1alpha suppression in myeloma cells blocks tumoral growth in vivo inhibiting angiogenesis and bone destruction. *Leukemia.* 2013;27(8):1697-1706.
34. Bai C, et al. SKP1 connects cell cycle regulators to the ubiquitin proteolysis machinery through a novel motif, the F-box. *Cell.* 1996;86(2):263-274.
35. Hoeck JD, et al. Fbw7 controls neural stem cell differentiation and progenitor apoptosis via Notch and c-Jun. *Nature neuroscience.* 2010;13(11):1365-1372.
36. Welcker M, et al. The Fbw7 tumor suppressor regulates glycogen synthase kinase 3 phosphorylation-dependent c-Myc protein degradation. *Proceedings of the National Academy of Sciences of the United States of America.* 2004;101(24):9085-9090.

37. Zhang W, Koepp DM. Fbw7 isoform interaction contributes to cyclin E proteolysis. *Molecular cancer research : MCR.* 2006;4(12):935-943.
38. Nguyen KD, et al. Circadian gene Bmal1 regulates diurnal oscillations of Ly6C(hi) inflammatory monocytes. *Science.* 2013;341(6153):1483-1488.
39. McCabe MT, et al. EZH2 inhibition as a therapeutic strategy for lymphoma with EZH2-activating mutations. *Nature.* 2012;492(7427):108-112.
40. Babaei-Jadidi R, et al. FBXW7 influences murine intestinal homeostasis and cancer, targeting Notch, Jun, and DEK for degradation. *The Journal of experimental medicine.* 2011;208(2):295-312.
41. N AG, et al. Phagocytosis imprints heterogeneity in tissue-resident macrophages. *The Journal of experimental medicine.* 2017;214(5):1281-1296.
42. Calderon-Gomez E, et al. Commensal-Specific CD4(+) Cells From Patients With Crohn's Disease Have a T-Helper 17 Inflammatory Profile. *Gastroenterology.* 2016;151(3):489-500 e483.
43. Friedrich M, Diegelmann J, Schauber J, Auernhammer CJ, Brand S. Intestinal neuroendocrine cells and goblet cells are mediators of IL-17A-amplified epithelial IL-17C production in human inflammatory bowel disease. *Mucosal immunology.* 2015;8(4):943-958.
44. Li H, et al. Genetic Deletion of Fbw7 in the mouse intestinal epithelium aggravated dextran sodium sulfate-induced colitis by modulating the inflammatory response of NF-kappaB pathway. *Biochemical and biophysical research communications.* 2018;498(4):869-876.
45. Amit I, Winter DR, Jung S. The role of the local environment and epigenetics in shaping macrophage identity and their effect on tissue homeostasis. *Nature immunology.* 2016;17(1):18-25.
46. Ventham NT, Kennedy NA, Nimmo ER, Satsangi J. Beyond gene discovery in inflammatory bowel disease: the emerging role of epigenetics. *Gastroenterology.* 2013;145(2):293-308.
47. Takeuch O, Akira S. Epigenetic control of macrophage polarization. *European journal of immunology.* 2011;41(9):2490-2493.
48. Nakanishi Y, Sato T, Takahashi K, Ohteki T. IFN-gamma-dependent epigenetic regulation instructs colitogenic monocyte/macrophage lineage differentiation in vivo. *Mucosal immunology.* 2018.
49. Li X, et al. Demethylase Kdm6a epigenetically promotes IL-6 and IFN-beta production in macrophages. *Journal of autoimmunity.* 2017;80:85-94.
50. Kruidenier L, et al. A selective jumonji H3K27 demethylase inhibitor modulates the proinflammatory macrophage response. *Nature.* 2012;488(7411):404-408.
51. McCabe MT, et al. Mutation of A677 in histone methyltransferase EZH2 in human B-cell lymphoma promotes hypertrimethylation of histone H3 on lysine 27 (H3K27). *Proceedings of the National Academy of Sciences of the United States of America.* 2012;109(8):2989-2994.
52. Liu Y, et al. Epithelial EZH2 serves as an epigenetic determinant in experimental colitis by inhibiting TNFalpha-mediated inflammation and apoptosis. *Proceedings of the National Academy of Sciences of the United States of America.* 2017;114(19):E3796-E3805.
53. Zhao E, et al. Cancer mediates effector T cell dysfunction by targeting microRNAs and EZH2 via glycolysis restriction. *Nature immunology.* 2016;17(1):95-103.
54. Best WR, Becktel JM, Singleton JW, Kern F, Jr. Development of a Crohn's disease activity index. National Cooperative Crohn's Disease Study. *Gastroenterology.* 1976;70(3):439-444.
55. Levesque BG, et al. Converging goals of treatment of inflammatory bowel disease from clinical trials and practice. *Gastroenterology.* 2015;148(1):37-51 e31.

56. Edgar RC, Haas BJ, Clemente JC, Quince C, Knight R. UCHIME improves sensitivity and speed of chimera detection. *Bioinformatics.* 2011;27(16):2194-2200.
57. Haas BJ, et al. Chimeric 16S rRNA sequence formation and detection in Sanger and 454-pyrosequenced PCR amplicons. *Genome research.* 2011;21(3):494-504.
58. Edgar RC. UPARSE: highly accurate OTU sequences from microbial amplicon reads. *Nature methods.* 2013;10(10):996-998.
59. Wirtz S, Neufert C, Weigmann B, Neurath MF. Chemically induced mouse models of intestinal inflammation. *Nature protocols.* 2007;2(3):541-546.
60. Bosma M, et al. FNDC4 acts as an anti-inflammatory factor on macrophages and improves colitis in mice. *Nature communications.* 2016;7:11314.
61. Qualls JE, Kaplan AM, van Rooijen N, Cohen DA. Suppression of experimental colitis by intestinal mononuclear phagocytes. *Journal of leukocyte biology.* 2006;80(4):802-815.
62. Bradley PP, Priebat DA, Christensen RD, Rothstein G. Measurement of cutaneous inflammation: estimation of neutrophil content with an enzyme marker. *The Journal of investigative dermatology.* 1982;78(3):206-209.
63. Boxio R, Bossenmeyer-Pourie C, Steinckwich N, Dournon C, Nusse O. Mouse bone marrow contains large numbers of functionally competent neutrophils. *Journal of leukocyte biology.* 2004;75(4):604-611.
64. Constantine CE, Wreghitt TG. A rapid micro-agglutination technique for the detection of antibody to Legionella pneumophila serogroup 5. *Journal of medical microbiology.* 1991;34(1):29-31.
65. Okayasu I, et al. A novel method in the induction of reliable experimental acute and chronic ulcerative colitis in mice. *Gastroenterology.* 1990;98(3):694-702.
66. Fukata M, et al. Toll-like receptor-4 promotes the development of colitis-associated colorectal tumors. *Gastroenterology.* 2007;133(6):1869-1881.
67. Lin W, et al. Raf kinase inhibitor protein mediates intestinal epithelial cell apoptosis and promotes IBDs in humans and mice. *Gut.* 2017;66(4):597-610.
68. Chen K, et al. Methyltransferase SETD2-Mediated Methylation of STAT1 Is Critical for Interferon Antiviral Activity. *Cell.* 2017;170(3):492-506 e414.
69. Polyak S, et al. Identification of adeno-associated viral vectors suitable for intestinal gene delivery and modulation of experimental colitis. *American journal of physiology. Gastrointestinal and liver physiology.* 2012;302(3):G296-308.

Figure 1

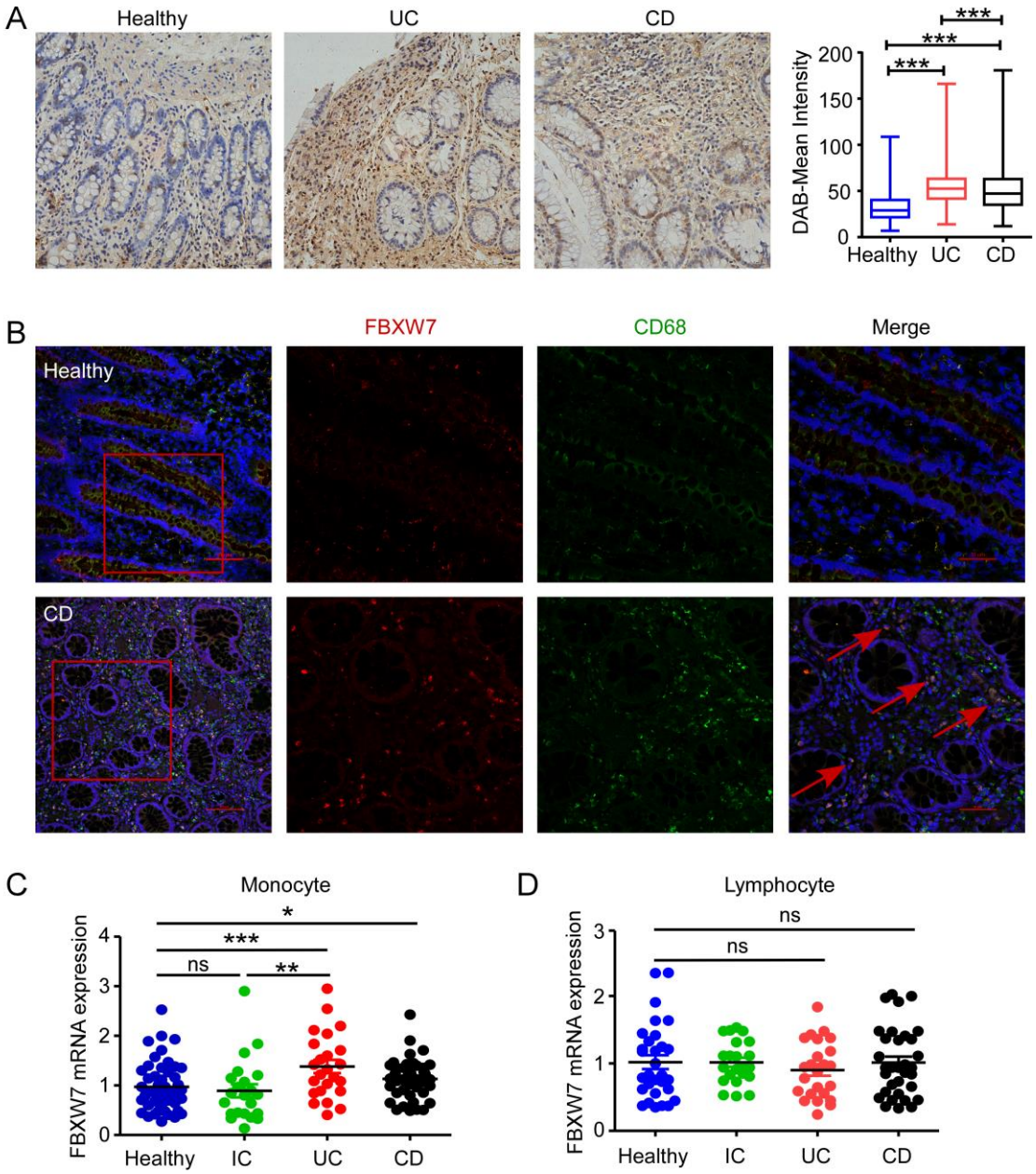

Figure 1. Increased FBXW7 expression in intestine inflammatory tissues in human. (**A**) Representative immunohistochemical (IHC) staining of paraffin sections of colon specimens obtained from colonic biopsies of patients with UC and CD, and healthy controls. Comparison of staining intensity (Tissue Gnostics) among the groups was shown. Original magnification, ×40. Scale bars, 50 μm. (**B**) Immunofluorescence staining for FBXW7 (red), CD68 (green) and DAPI for nuclei (blue) in human healthy and CD tissues. Scale bars, 100 μm (whole colon section) or 50 μm (detail). *FBXW7* mRNA expression in peripheral blood monocytes (**C**) of healthy controls (n=50), IC (n=22), UC (n=24) and CD (n=44) patients or in peripheral blood lymphocytes (**D**) from patients with IC (n=22), UC (n=24), CD (n=33) and healthy controls (n=30). Statistical significance was assessed by one-way ANOVA with Tukey's multiple comparisons test; *p<0.05, **p<0.01, ***p<0.001. Data are presented as mean ± SEM and representative of three independent experiments. UC, ulcerative colitis; CD, Crohn's disease; IC, non-IBD inflammation control (acute diarrhea).

Figure 2

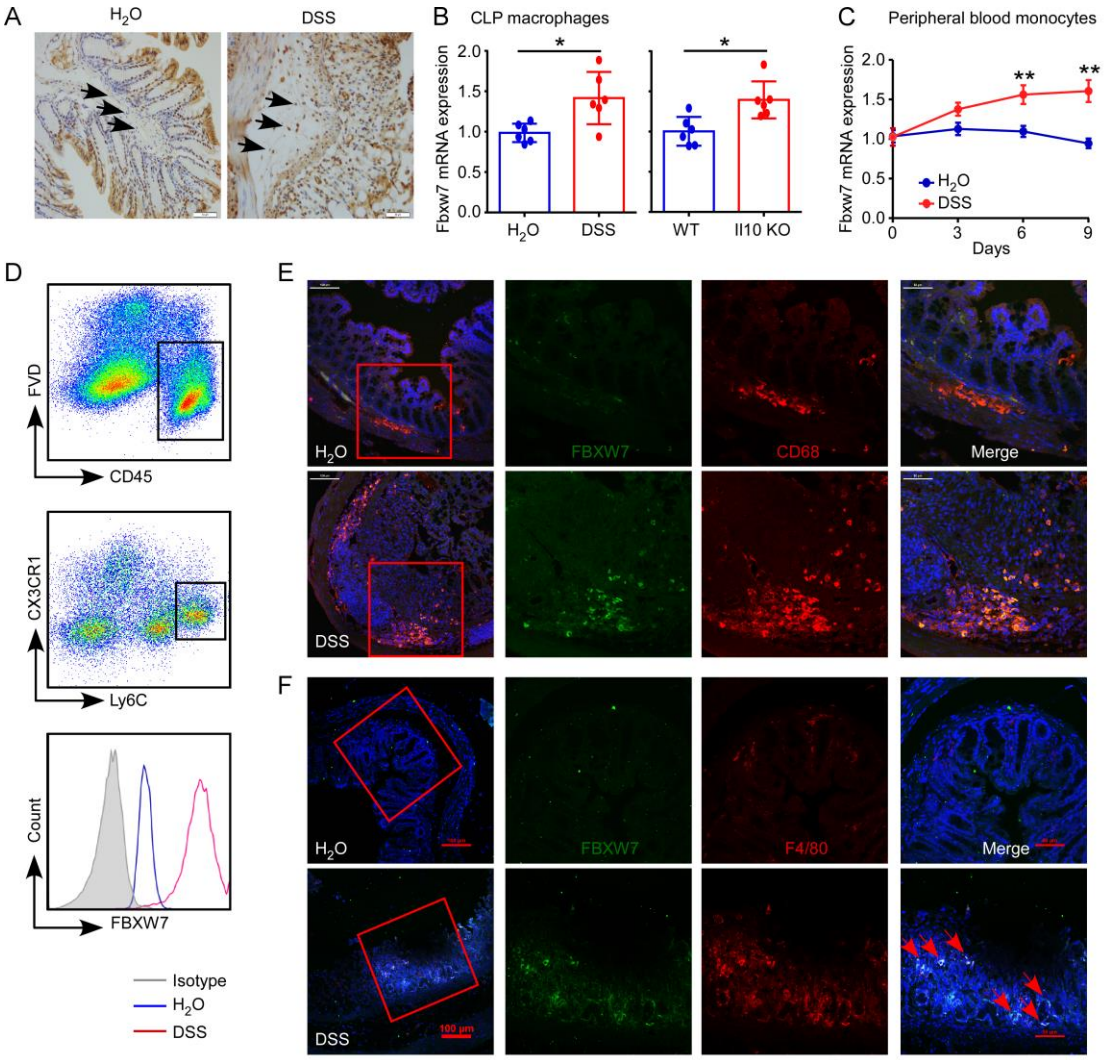

Figure 2. Increased Fbxw7 expression in intestine inflammatory tissues in mice. (**A**) Representative IHC staining of colon specimens obtained from control and colitis mice with 5 days DSS treatment. Scale bars, 50 μm (**B**) *Fbxw7* mRNA expression in CLP CD11b^{+}CX3CR1^{+} macrophages of DSS-induced colitis (day 9) mice and 12-week old *Il-10*$^{-/-}$ mice (n=6). (**C**) Quantitative assessment of *Fbxw7* mRNA expression in peripheral blood monocytes from mice with colitis at different timepoints after DSS attack (n=6). (**D**) Representative flow cytometric analysis of FBXW7 expression in mice Ly6C^{hi}CX3CR1^{int} colonic monocytes at steady and inflammation status. Immunofluorescence staining for (**E**) FBXW7 (green), CD68 (red) and DAPI for nuclei (blue) and (**F**) FBXW7 (green), F4/80 (red) and DAPI for nuclei (blue) in mice colonic tissues from control and DSS-colitis mice. Scale bars, 100 μm (whole colon section) or 50 μm (detail). Statistical significance was assessed by unpaired two-tailed Student's *t* test; *p<0.05, **p<0.01. Data are presented as mean ± SD from at least three independent experiments. DSS, dextran sulfate sodium; *Fbxw7*, F-box and WD repeat domain-containing 7. FVD, Zombie Violet™ Fixable Viability Dye.

Figure 3

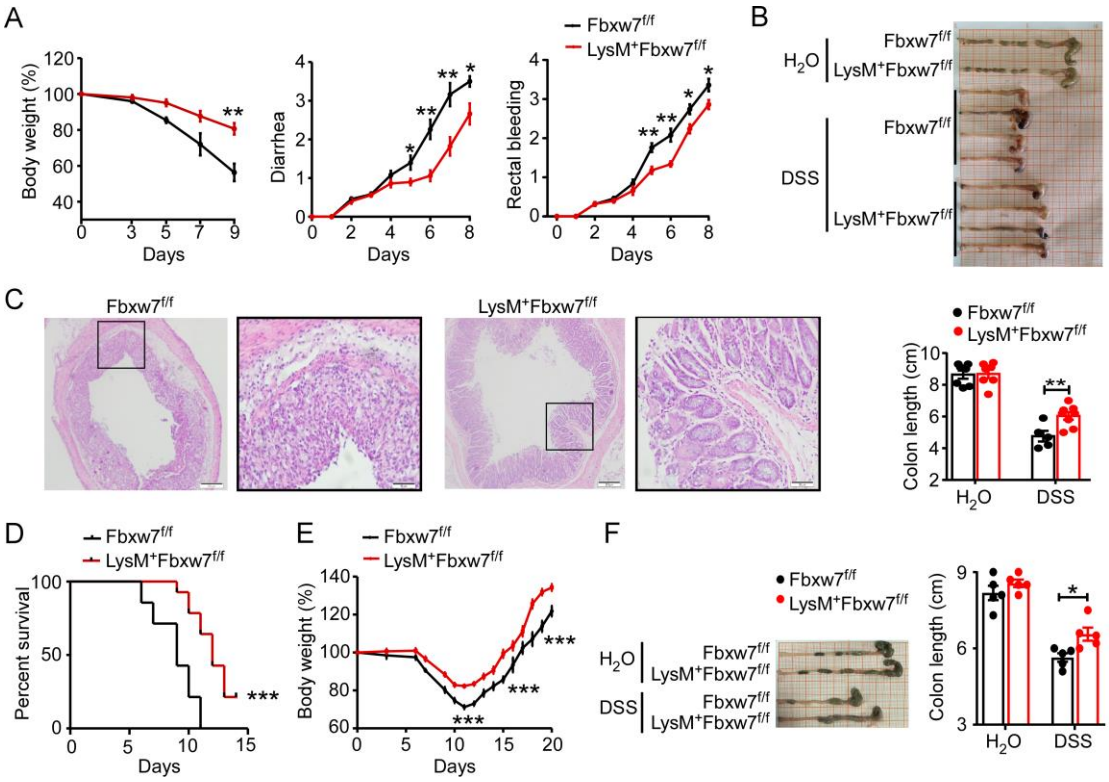

Figure 3. *LysM⁺Fbxw7$^{f/f}$* mice showed attenuated experimental colitis. *Fbxw7$^{f/f}$* and *LysM⁺Fbxw7$^{f/f}$* mice were administered with water or 3% DSS for 7 days to induce acute colitis and followed by 2 days recovery on normal drinking water. Body weight change, diarrhea and rectal bleeding score (**A**) were assessed daily as described in the 'methods' (n=5). (**B**) Gross morphology images of the colon from *Fbxw7$^{f/f}$* or *LysM⁺Fbxw7$^{f/f}$* mice, and colon length were measured on day 9 (n≥5). (**C**) H&E staining of colonic sections, scale bars, 200 μm (whole colon section) and 50 μm (detail). (**D**) *Fbxw7$^{f/f}$* and *LysM⁺Fbxw7$^{f/f}$* mice were administered with 4% DSS to induce acute colitis. Mice death was monitored until day 15 (n=10). Log-rank test, **p<0.01. (**E**) Body weight change during the process of intestinal inflammation and recovery period (n=5). (**F**) Colon length of *Fbxw7$^{f/f}$* and *LysM⁺Fbxw7$^{f/f}$* mice sacrificed after 7 days 3% DSS treatment and 8 days' recovery with drinking water (n=5). Data are presented as mean ± SEM and representative of three independent experiments. Statistical significance was assessed by unpaired two-tailed Student's *t* test; *p<0.05, **p<0.01, ***p<0.001.

Figure 4

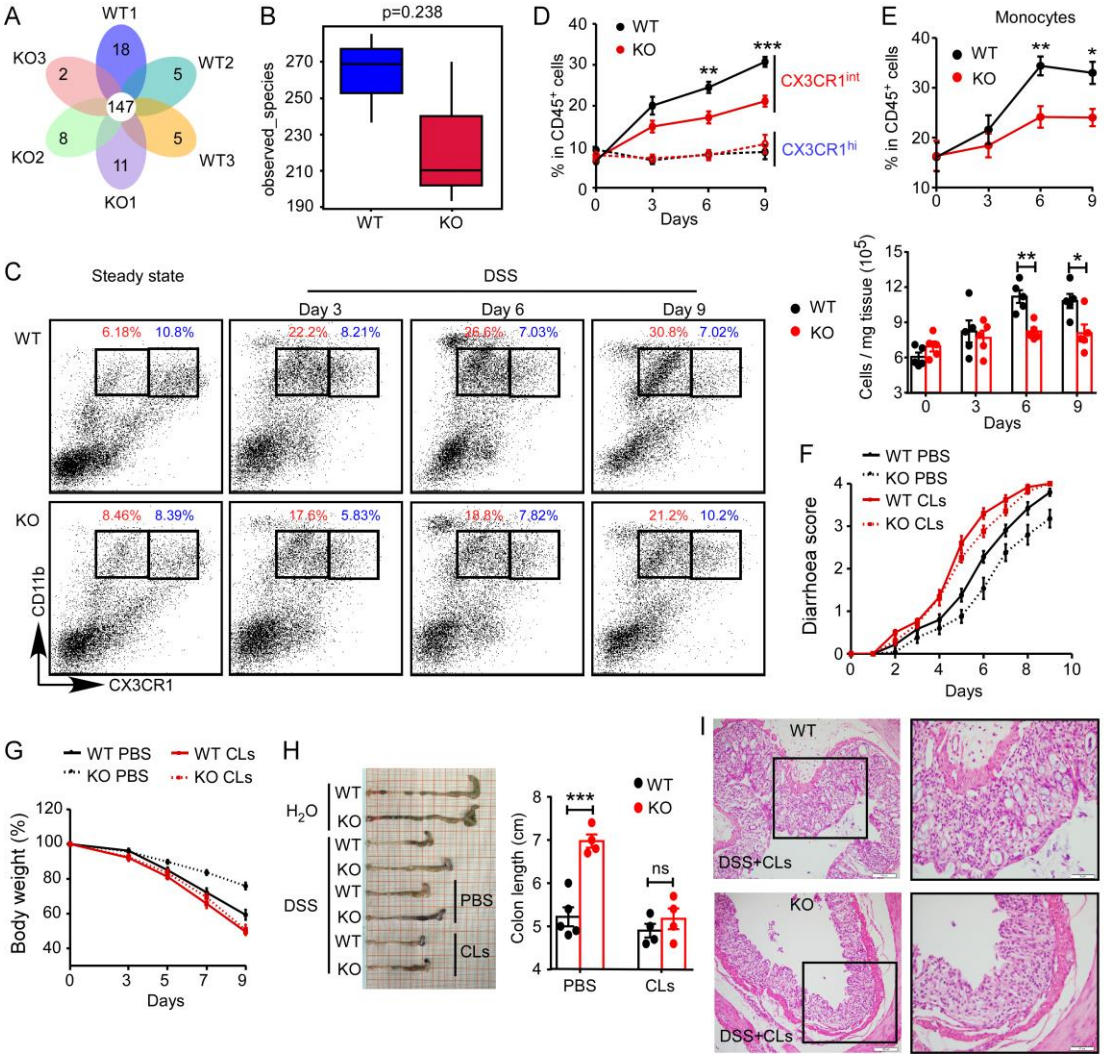

Figure 4. *Fbxw7* deficiency decreases the accumulation of CX3CR1^{int} pro-inflammatory MPh. (**A**) Venn diagram of *Fbxw7$^{f/f}$* (WT) and *LysM^{+}Fbxw7$^{f/f}$* (KO) groups showing unique and shared OTUs for bacterial sequences based on normalized sequences and 97% sequence similarity (n=3). (**B**) The analysis of alpha-diversity (observed_species) in WT and KO groups (n=3), p value was calculated from the analysis of independent-samples Student's *t* test. (**C**) Representative flow cytometry plots gated on CD45^{+} living cells isolated from CLP of WT and KO mice on days 0, 3, 6, 9 after DSS challenge. CD11b^{+}CX3CR1^{hi} resident macrophages (blue), CD11b^{+}CX3CR1^{int} MPh (red). (**D**) Dynamics of CD11b^{+}CX3CR1^{hi} macrophages, CD11b^{+}CX3CR1^{int} MPh infiltration in CLP after DSS treatment (n=5 for any time point). (**E**) The percentages and number of Ly6C^{hi}CX3CR1^{int} monocytes in the flamed colon after DSS treatment (n=5 for any time point). Then, macrophages were depleted by clodronate-containing liposomes in WT and KO mice and subjected to 3% DSS treatment for 7 days; mice were sacrificed on day 9. Diarrhea score (**F**) and body weight change (**G**) were assessed daily (n=5). (**H**) Gross morphology images of the colon from mice at day 9 after DSS treatment and colon length was measured (n=5). (**I**) Colonic sections were analyzed by H&E staining of colitis mice. Scale bars, 200 μm (whole colon section) and 50 μm (detail). CLs, clodronate-containing liposomes. **(C-H)** Data are expressed as mean ± SEM from at least three independent experiments. Statistical significance was assessed by unpaired two-tailed Student's *t* test; *p<0.05, **p<0.01, ***p<0.001.

Figure 5

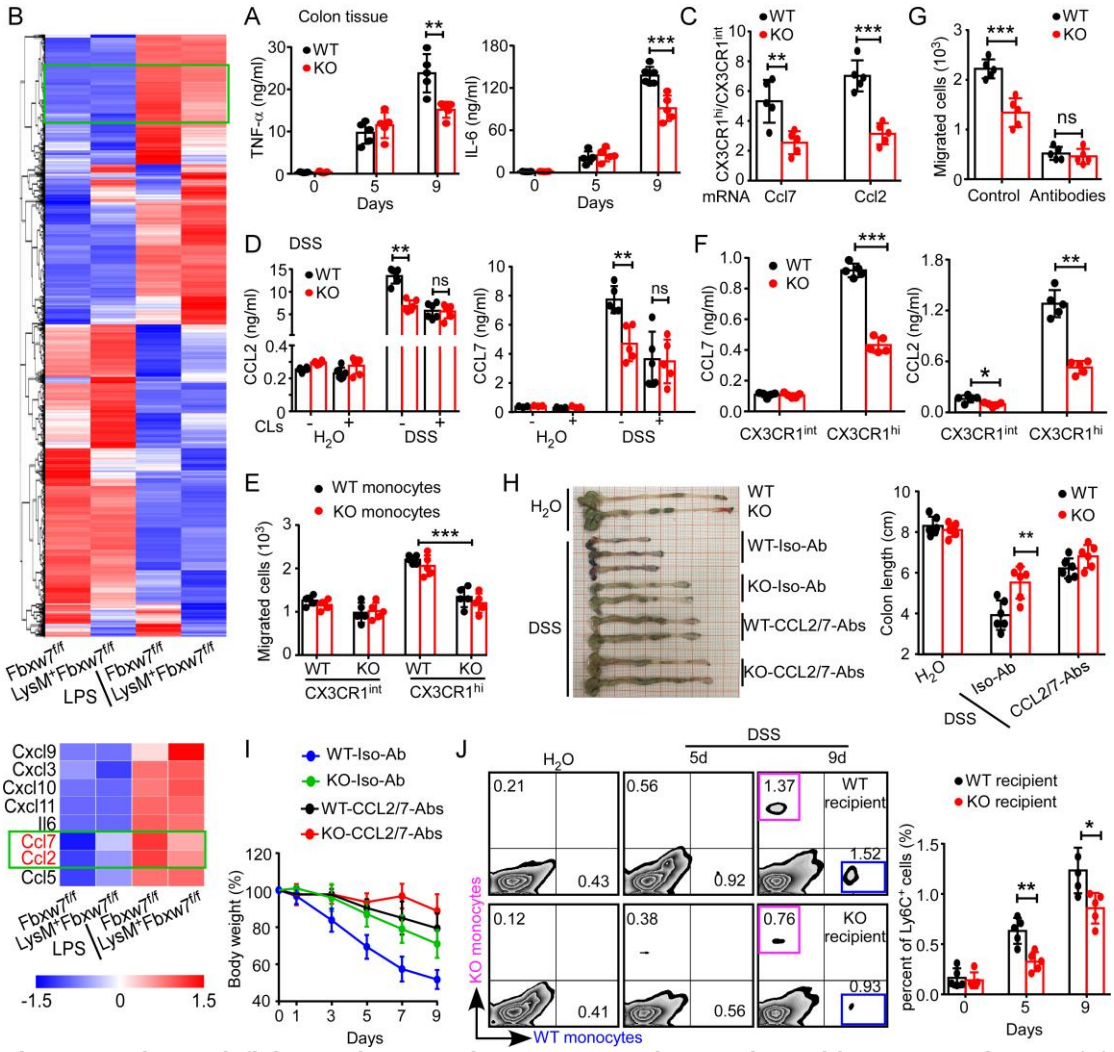

Figure 5. *Fbxw7* deficiency downregulates CCL2 and CCL7 in resident macrophages. (**A**) Colonic tissue was cultured overnight, cytokines in the supernatant were measured by ELISA (n=5). (**B**) Heat map showing expression changes of inflammation related genes in BMDMs from *LysM*$^{+}$*Fbxw7*$^{f/f}$ mice and *Fbxw7*$^{f/f}$ littermates. Expression profile is accompanied by a colored bar indicating the standardized log 2 intensities. BMDMs were isolated from *LysM*$^{+}$*Fbxw7*$^{f/f}$ mice and *Fbxw7*$^{f/f}$ littermates and stimulated with LPS (100 ng/ml) for transcriptome assay. (**C**) CD11b^{+}CX3CR1^{hi} resident macrophages and CD11b^{+}CX3CR1^{int} pro-inflammatory MPh were sorted from CLP of *Fbxw7*$^{f/f}$ (WT) and *LysM*$^{+}$*Fbxw7*$^{f/f}$ (KO) mice (n=5) after 5-day DSS or H_2O administration, gene expressions were quantified by gene specific amplification and qRT-PCR, the ratio of *Ccl2* and *Ccl7* expression in CX3CR1^{hi} resident macrophages to those in CX3CR1^{int} MPh was shown. (**D**) Colonic tissues of WT and KO mice treated with DSS were cultured overnight, CCL2/CCL7 in the supernatant were measured by ELISA (n=5). (**E**) In transwell assay, the number of monocytes in lower chamber recruited by supernatant of CLP-derived CX3CR1^{hi} resident macrophages and CX3CR1^{int} pro-inflammatory MPh were counted by cytometry (n=5). (**F**) The concentration of CCL2 and CCL7 in the culture medium of CX3CR1^{hi} macrophages and CX3CR1^{int} MPh (n=5). (**G**) The number of monocytes in lower chamber recruited by supernatant of CX3CR1^{hi} resident macrophages of WT mice with or without CCL2/7 antibodies (n=5). (**H**) Gross morphology images of the colon from *Fbxw7*$^{fl/fl}$ or *LysM*$^{+}$*Fbxw7*$^{fl/fl}$ mice with or without anti-CCL2/7 Ab, and colon length were measured on day 9 (n=5). (**I**) Body weight change was assessed daily (n=5). (**J**) The percentages of labeled WT and KO monocytes gated on CD45^{+}Ly6C^{hi} living cells were analyzed by flow cytometry in DSS-challenged recipient mice (n=5), and graphical summary of the percentages of labeled WT monocytes recruited to the CLP of WT and KO recipient mice at day 5 or 9 after DSS onset. Data are presented as mean ± SD and representative of three independent experiments. Statistical significance was assessed by unpaired two-tailed Student's *t* test; *p<0.05, **p<0.01, ***p<0.001.

Figure 6

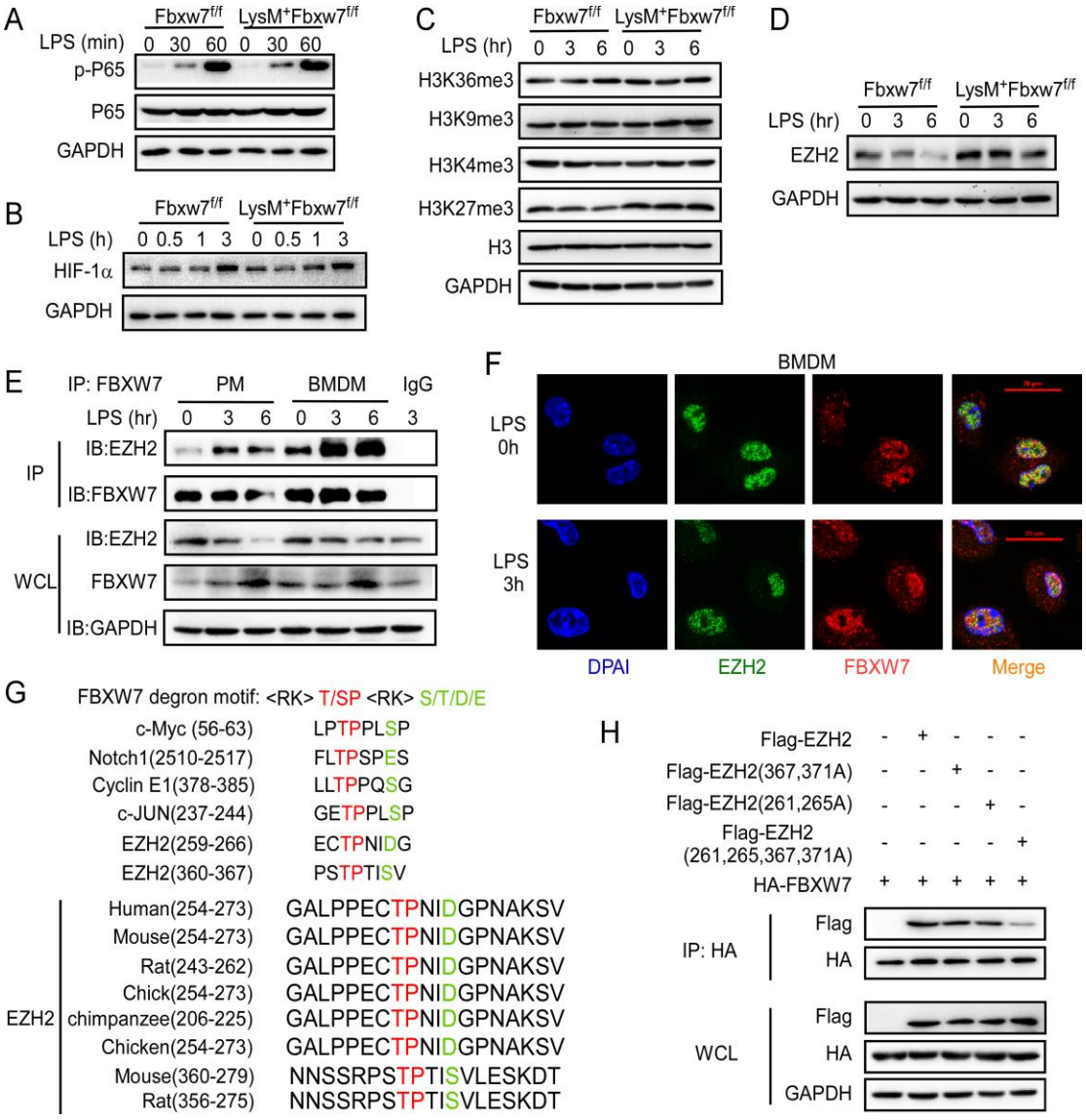

Figure 6. FBXW7 interacts with EZH2. Immunoblot analysis of phosphorylated and total proteins of P65 (**A**), HIF-1α (**B**), H3 histone modification (**C**) and histone methyltransferase EZH2 protein level (**D**) in lysates of bone marrow-derived macrophages (BMDMs) from *Fbxw7$^{f/f}$* and *LysM^{+}Fbxw7$^{f/f}$* mice stimulated for indicated hours with LPS. (**E**) Co-immunoprecipitation and immunoblot of BMDMs stimulated with LPS for indicated hours. (**F**) Confocal microscopic imaging of BMDMs that stimulated with LPS and labeled with antibodies to the appropriate protein. (**G**) Sequence alignment of EZH2 with FBXW7 degron motif (< RK >S/TP < RK > XS/T/E/D), where X and < RK > are any amino acid, except arginine (R) or lysine (K). (**H**) Coimmunoprecipitation and immunoblot analysis of HEK293T cells transfected with HA-FBXW7 along with vector for Flag-EZH2 (WT), Flag-EZH2 (261A and 265A), Flag-EZH2 (367A and 371A) and Flag-EZH2 (261A and 265A, 367A and 371A) (4A) and treated with MG132, followed by immunoprecipitation with anti-HA-M2 beads. All data are representative of at least three independent experiments.

Figure 7

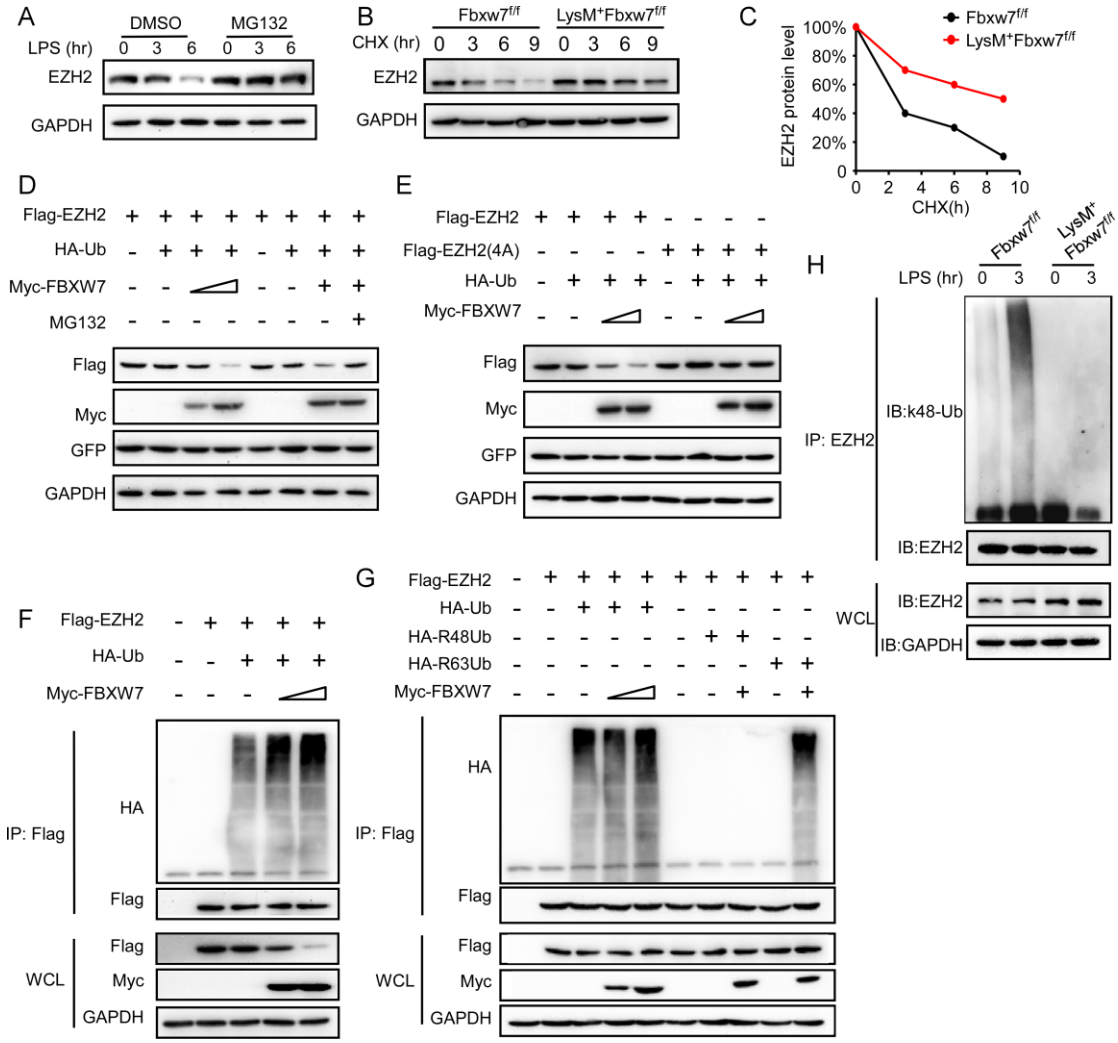

Figure 7. FBXW7 mediates the ubiquitination of EZH2 in macrophages. (**A**) Immunoblot analysis of EZH2 expression in BMDMs treated with or without MG132 for 8 hours and stimulated with LPS for indicated hours. (**B**) Immunoblot analysis of EZH2 in lysates of *Fbxw7*$^{f/f}$ and *LysM*$^{+}$*Fbxw7*$^{f/f}$ BMDMs treated with CHX (40 μg/ml) for indicated hours after stimulation with LPS for 1 hour. (**C**) Quantification of relative EZH2 protein levels is shown. (**D**) Immunoblot analysis of HEK293T cells cotransfected for 36 hours with Myc-FBXW7, plus Flag-EZH2, HA-Ub and GFP vectors treated with or without MG132. (**E**) Immunoblot analysis of HEK293T cells cotransfected for 36 hours with Myc-FBXW7, HA-Ub and GFP, along with vector for Flag-EZH2, Flag-EZHh2 (261, 265, 367 and 371A, 4A). (**F**) Immunoblot analysis of the ubiquitination of EZH2 in HEK293T cells cotransfected with Flag-EZH2, HA-Ub, along with increasing concentrations (wedge) of vectors for the Myc-FBXW7 constructs and treated with MG132 for 6 hours before harvest. (**G**) Immunoblot analysis of the ubiquitination of EZH in HEK293T cells cotransfected with Flag-EZH2, Myc-FBXW7 along with HA-Ub, the mutant ubiquitin HA-R48 Ub or HA-R63 Ub and treated with MG132 before cell harvest. (**H**) Immunoblot analysis of the K48 ubiquitination of EZH2 in *Fbxw7*$^{f/f}$ and *LysM*$^{+}$*Fbxw7*$^{f/f}$ BMDMs stimulated with LPS. All data are representative of at least three independent experiments.

Figure 8

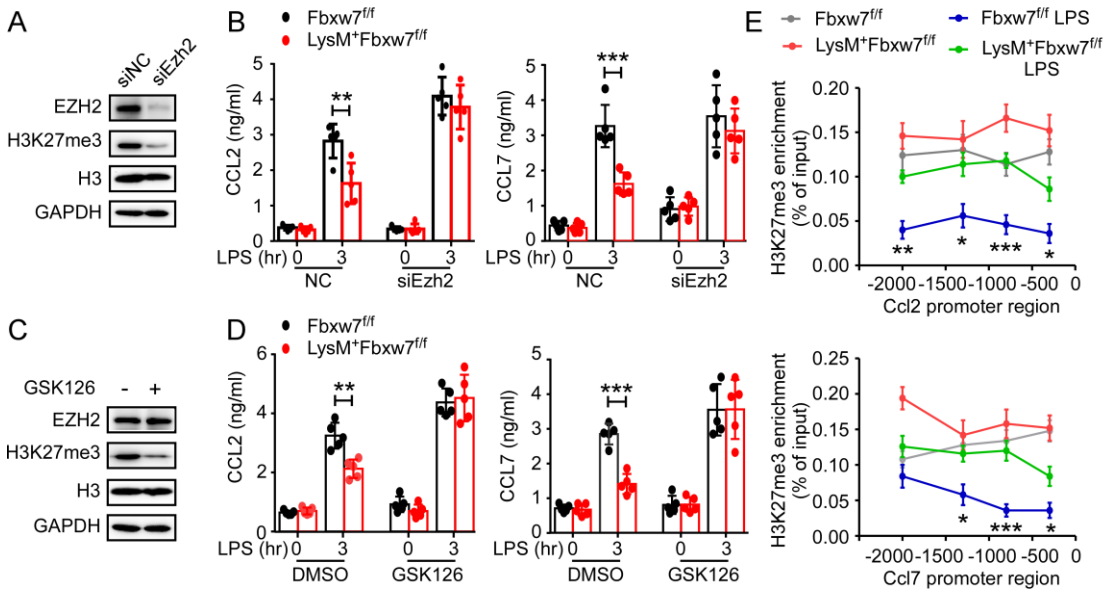

Figure 8. EZH2 inhibits macrophage *Ccl2* and *Ccl7* expression through H3K27me3 modification. (**A**) *Ezh2* in BMDMs was silenced with control small interfering RNA (siNC) or *Ezh2*-specific siRNA (siEzh2) for 48 hours, effects of siEzh2 on *Ezh2* expression and H3K27me3 modification in BMDMs were analyzed by immunoblot. (**B**) The concentration of CCL2 and CCL7 in the culture medium of *Fbxw7$^{f/f}$* and *LysM^{+}Fbxw7$^{f/f}$* BMDMs after siEzh2 and LPS treatment were quantified by ELISA (n=5). (**C**) 10 μM GSK126 or DMSO were added into the cell culture medium for 2 days, the levels of EZH2, H3K27me3, H3 were detected with immunoblot. (**D**) The concentration of CCL2 and CCL7 in the culture medium of *Fbxw7$^{f/f}$* and *LysM^{+}Fbxw7$^{f/f}$* BMDM after GSK126 and LPS treatment were quantified by ELISA (n=5). (**E**) ChIP assay of enrichment of H3K27me3 on promoters of *Ccl2* and *Ccl7* in BMDMs followed by LPS treatment. Data are presented as mean ± SD and representative of at least three independent experiments. Statistical significance was assessed by unpaired two-tailed Student's *t* test; *p<0.05, **p<0.01, ***p<0.001.

Figure 9

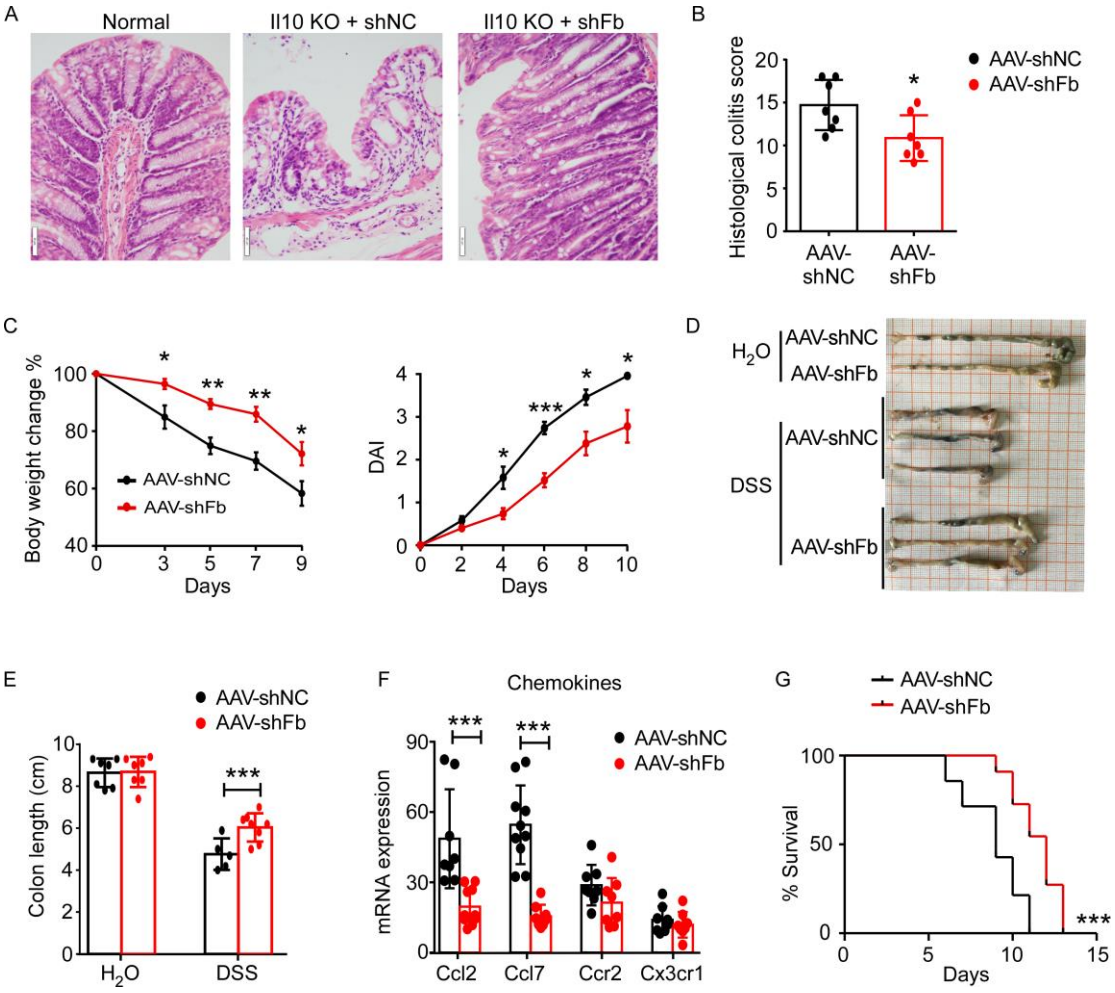

Figure 9. Decreased expression of *Fbxw7* relieved experimental colitis. (**A**) H&E staining of colonic sections from 12-week old *Il10*$^{-/-}$ mice injected with AAV weekly from 5-week age until 9-week old (n=7) and its histopathological scores (**B**) were assessed. Scale bars, 50 μm. (**C**) Body weight change and active disease index of healthy control and DSS-induced colitis C57BL/6 mice were assessed daily (n=5). (**D**) Gross morphology images of the colon from healthy and colitis mice sacrificed on day 9 and colon length (**E**) was measured (n=7). (**F**) The colon tissue mRNA from mice sacrificed on day 7 were subjected to determine the mRNA expression of chemokines and its ligand (n≥6). Data are presented as mean ± SD and representative of at least three independent experiments. Statistical significance was assessed by unpaired two-tailed Student's *t* test; *p<0.05, **p<0.01, ***p<0.001. (**G**) AAV-shNC and AAV-shFB mice were administered with 4% DSS to induce acute colitis. Mouse death was monitored until day 15 (n=5). Log-rank test, **p<0.01. Data are representative of three independent experiments.